RSC Advances

REVIEW

View Article Online
View Journal | View Issue

Cite this: *RSC Adv.*, 2026, **16**, 16631

Lanthanide ion-doped carbon dots (Ln-CDs) as fluorescent nanoprobes: a review

Kawan F. Kayani * and Rebaz F. Hamarawf

Breakthroughs in nanoscale science and engineering have facilitated the design of nanomaterials with exceptional optical behaviors. Over the past decade, numerous fluorescent nanoprobes have been reported for the highly sensitive and selective detection of a wide range of analytes. Among these, doped carbon dots (CDs) have become a major focus of researchers across multiple disciplines due to their exceptional physicochemical and optical properties. Lanthanide ion-doped carbon dots (Ln-CDs) have attracted increasing attention in recent years as specialized nanoprobes for luminescent detection because of their unique optical behavior, chemical stability, and low toxicity. However, most existing studies are limited to luminescence color modulation under different excitation wavelengths, and only a few reports have exploited dual-emission sources for nanoprobe construction. This review summarizes lanthanide-ion-doped carbon dots, highlighting the unique roles of lanthanide ions, doping mechanisms, and their advantages for analytical applications. In addition, the applications of these nanoprobes in various fields, including metal-ion detection, pharmaceutical analysis, contaminant monitoring, anthrax biomarker detection, and biomolecule sensing, are systematically discussed. In summary, Ln-CD-based nanoprobes show potential as promising candidates for future analytical platforms for the detection of multiple analytes.

Received 22nd February 2026
Accepted 13th March 2026

DOI: 10.1039/d6ra01564f

rsc.li/rsc-advances

1. Introduction

Chemical sensors play important roles in various fields including chemistry, biology, medical diagnostics, and environmental science.[1–4] Typically, these sensors contain receptors that convert chemical interactions into measurable analytical signals when they bind with specific target species.[5] Numerous techniques have been developed for the sensitive detection of analytes, including atomic absorption spectroscopy (AAS),[6] inductively coupled plasma mass spectrometry (ICP-MS),[7] electrochemical sensing,[8] chemiluminescence sensing,[9] and fluorescence (FL)-based sensing. The fluorescence sensing strategy is prevalent, as it is an easy-to-use, low-cost, and sensitive method that enables real-time online detection.[10] Researchers have exploited many kinds of fluorescent nanomaterials to detect multiple analytes, including nanoclusters (NCs),[11,12] semiconductor quantum dots,[13,14] metal–organic frameworks (MOFs),[15,16] covalent organic frameworks (COFs),[17] sulfur dots,[18] nanocomposite fluorescent sensors,[19,20] and CDs.[21]

Despite their advantages, the previously reported sensors still exhibit several limitations. These drawbacks include the need for complex modifications in hybrid fluorescent dyads and the relatively high cost associated with gold and silver nanoclusters.[22] For example, MOFs often demonstrate limited chemical selectivity,[23] while COFs and near-infrared nanosensors typically involve complicated and time-consuming synthesis procedures.[24] In addition, quantum dots (QDs) may present potential toxicity due to the presence of metal ions, and NCs generally suffer from poor stability.[25] Consequently, there is a significant need to develop fluorescent nanoprobes that are simple and cost-effective and provide rapid responses.

Selecting appropriate fluorescent materials is crucial for their application as sensors for various analytes, including metal ions,[26,27] anions,[28] drugs,[29] biomarkers,[30] and pollutant detection.[31] CDs are promising fluorescent sensors because of their readily available and widely distributed precursor sources, good water solubility, strong and stable FL, good biocompatibility, low toxicity, and ease of preparation.[32] In addition, CDs are a novel family of fluorescent nanomaterials that are usually less than 10 nm in size.[33] Since their discovery in 2004, CDs have attracted significant attention owing to their superior photostability, water solubility, and resistance to photobleaching.[34–36]

Because of these characteristics of CDs, they are widely used in a variety of fields. There are two primary methods for creating CDs: "top-down" and "bottom-up". Larger carbon structures are broken down by top-down techniques, including ball milling,[37] chemical exfoliation,[38] and ultrasonic treatment,[39] which are helpful for large-scale production. However, they frequently entail challenging conditions, protracted processing periods, and costly equipment. By contrast, more popular bottom-up

Department of Chemistry, College of Science, University of Sulaimani, Qliasan St, Sulaimani City, 46002, Kurdistan Region, Iraq. E-mail: kawan.nasralddin@univsul.edu.iq

approaches involve chemical vapour deposition,[40] hydrothermal treatment,[41] and microwave pyrolysis[42] to create CDs from small molecular precursors. These methods generally yield CDs with fewer defects and allow better control over the final outcome.[43,44]

In semiconductor research, doping is a fundamental technique for precisely tuning a material's optical, magnetic and electrical properties. The atomic orbitals of heteroatoms can overlap with those of carbon atoms when they are introduced in CDs' nanostructure. This interaction can have a significant impact on the electronic structure, morphology, and chemical composition of CDs when combined with the electron-withdrawing or -donating characteristics of the heteroatoms.[45] The incorporation of nonmetallic heteroatoms such as N, S, B and P is common in most doped CDs reported to date.[46] Metal ions are able to cause even more pronounced changes because of their greater number of electrons, larger atomic radii, and available orbitals. The electrostatic distribution and energy bandgap of CDs can be fine-tuned by doping them with metal ions, which greatly alters their physical and chemical properties.[47,48]

Although various metal ions, such as Fe, Ni, Mn, and Cu, are used for doping carbon dots, nonfluorescent metal-ion-doped CDs generally do not introduce new emission peaks. Instead, they influence FL indirectly by modifying surface states or electron density, resulting in intensity-based turn-on/off sensing. The main advantages of fluorescent metal-doped CDs are their simplicity, cost-effectiveness, and suitability for general sensing or photostability enhancement,[48–52] whereas their main disadvantage is the lack of intrinsic FL. In contrast, lanthanide ions exhibit remarkable spectral features, including long-lived excited states, a large Stokes shift, and narrow emission bands.[53,54] Lanthanide-based luminescent materials are widely employed in chemical and biological sensing systems because of their strong and selective responses to specific analytes.[55] These materials have been extensively studied due to their unique optical properties. However, generating FL through direct excitation is challenging because the f–f transitions of lanthanide ions (Ln^{3+}) are forbidden. The antenna effect addresses this issue: when chromophore-containing ligands bind to Ln^{3+}, they form lanthanide complexes that enhance luminescence through efficient energy transfer.[56] Therefore, Ln^{3+} coupled with CDs is highly promising for fluorescent sensing applications owing to its simple preparation, long-wavelength emissions, multiple emission bands and the large Stokes shift characteristic of fluorescent Ln^{3+}.

Recently, several reviews on the properties, characterization, and various technological applications of CDs have been published. However, a focused review on lanthanide ion-doped CDs in promising analytical applications is still lacking in the literature. Therefore, in this review, we first introduce CDs and their properties and then discuss lanthanide ion-doped CDs and their functionalization mechanisms. As shown in Fig. 1, these observations provide a clearer understanding of the differences between undoped CDs and lanthanide ion-doped CDs, and finally, we describe their applications in diverse fields as fluorescent nanoprobes.

1.1 Novelty statement

Based on a search on lanthanide ion-doped CDs, the first publication on this topic appeared in 2011 by Zhao *et al.*,[57] who explored europium-doped CDs for the detection of phosphate in complex matrices. Since then, publications on this topic have increased, with most lanthanide ions being chosen for doping or coordination with CDs for various purposes. In this review, for the first time, all relevant articles on lanthanide ion-doped CDs used as fluorescent nanoprobes are compiled and evaluated with respect to their properties and the types of bonding between lanthanide ions and CDs. In addition, the applications of these fluorescent nanoprobes in various fields, including

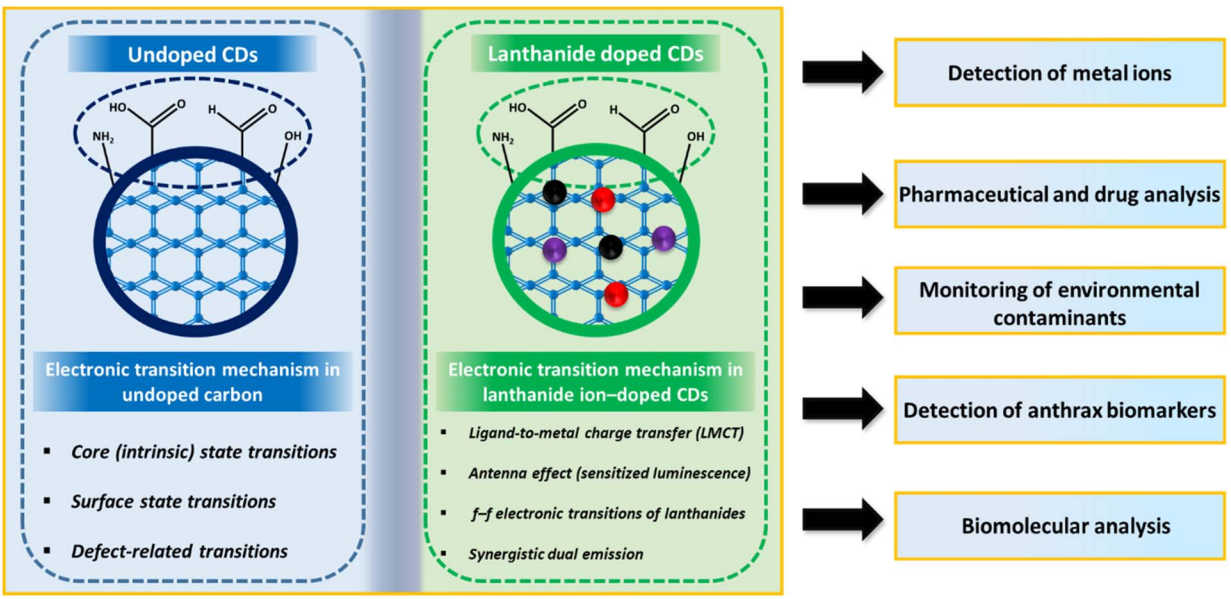

Fig. 1 Comparison between undoped CDs and Ln-CDs.

Table 1 Comparison of this work with previous studies on doped CDs

Types of dopants	Summary of published works on doped carbon dots	Year of publication	Ref.
Heteroatom	Li *et al.* published a study on non-metal heteroatom-doped carbon dots, focusing on their synthesis and properties, without discussing their applications	2018	58
Heteroatom	Miao *et al.* published a review article on heteroatom-doped carbon dots, discussing doping strategies and applications, including optoelectronic devices, nano-probes, catalysis, and biomedicine	2020	59
Metal	Li *et al.* published a review article on metal-doped carbon dots, focusing on their synthesis methods and applications in sensing, optoelectronics, imaging, phototherapy, and catalysis	2022	60
Nitrogen	Munusamy *et al.* published a review on nitrogen-doped carbon dots and their applications as fluorescent sensors	2023	61
Boron	Fu *et al.* published a review on boron-doped carbon dots, discussing their doping strategies, performance effects, and applications in information encryption, optical sensors, and anti-counterfeiting	2024	62
Nitrogen	Mohammed *et al.* published a review on nitrogen-doped carbon dots and their applications for anti-bacterial purposes	2025	46
Phosphorus	Kayani *et al.* published work focusing on phosphorus-doped carbon dots and their applications in analytical and bioanalytical fields	2025	63
Lanthanides	As mentioned above, no review has specifically focused on lanthanide ion-doped carbon dots as fluorescent nanoprobes. Based on the literature survey, this topic is considered novel and unique	2026	This work

metal-ion detection, pharmaceutical analysis, contaminant monitoring, anthrax biomarker detection, and biomolecule sensing, are systematically discussed. In summary, lanthanide ion-doped carbon dot-based nanoprobes demonstrate strong potential as promising candidates for future analytical platforms for the detection of multiple analytes. Table 1 discusses the main differences between this work and previously published reviews on doped CDs, particularly in terms of their applications.

2. Advantages of lanthanide ion-doped carbon dots

Lanthanides, also known as lanthanoids, comprise a group of elements located in the f-block at the bottom of the periodic table.[64] This block is defined by the presence of f electrons, which play a crucial role in determining the chemical behavior of these elements. Although commonly referred to as "rare-earth elements", lanthanides are actually more abundant in the Earth's crust than gold. For many years, they attracted relatively limited attention; however, beginning in the 1980s, interest in lanthanide chemistry has increased significantly, leading to rapid advances in the field.[65,66] This renewed focus is largely attributed to the unique characteristics of their 4f electrons, which endow lanthanides with exceptional optical and magnetic properties that are now widely exploited in various commercial technologies.[67] In solution, lanthanide chemistry is predominantly governed by the +3 oxidation state under oxygen-rich conditions, a feature that initially contributed to the limited exploration of these elements.[68] Notable exceptions occur for ions with empty, half-filled, or completely filled 4f subshells. A representative example is Eu(II), whose half-filled

Table 2 Summary of all lanthanide elements

Element	Symbol	Atomic number	4f Configuration (Ln^{3+})	Characteristic optical properties
Lanthanum	La^{3+}	57	$4f^0$	No f–f emission
Cerium	Ce^{3+}	58	$4f^1$	Broad UV-blue (5d–4f)
Praseodymium	Pr^{3+}	59	$4f^2$	Green-red emissions
Neodymium	Nd^{3+}	60	$4f^3$	Near-IR emission
Promethium	Pm^{3+}	61	$4f^4$	Weak emission
Samarium	Sm^{3+}	62	$4f^5$	Orange-red emission
Europium	Eu^{3+}	63	$4f^6$	Intense-red emission
Gadolinium	Gd^{3+}	64	$4f^7$	No visible emission
Terbium	Tb^{3+}	65	$4f^8$	Strong-green emission
Dysprosium	Dy^{3+}	66	$4f^9$	Blue-yellow emission
Holmium	Ho^{3+}	67	$4f^{10}$	Green emission
Erbium	Er^{3+}	68	$4f^{11}$	Green and IR emissions
Thulium	Tm^{3+}	69	$4f^{12}$	Blue emission
Ytterbium	Yb^{3+}	70	$4f^{13}$	Near-IR emission
Lutetium	Lu^{3+}	71	$4f^{14}$	No f–f emission

$4f^7$ electronic configuration provides enhanced stability to the +2 oxidation state under reducing environments. Although most lanthanides have since been stabilized in the divalent state through advances in organometallic chemistry, these species typically require carefully designed ligands and can only be maintained under controlled atmospheric conditions.[67] Despite their sharp and characteristic emission features, Ln^{3+} ions exhibit inherently weak light absorption because of the Laporte-forbidden nature of the f–f electronic transitions. As a result, the molar absorption coefficients of most Ln^{3+} ions are very low, and only a limited fraction of incident radiation can be absorbed through the direct excitation of the 4f energy levels. This drawback can be mitigated by coordinating Ln^{3+} ions with organic ligands capable of efficient light absorption and energy transfer (ET) processes, commonly referred to as the "antenna effect" or "luminescence sensitization". The resulting luminescence behavior is governed by the efficiency of energy transfer from the ligand (antenna) to the Ln^{3+} ion (emissive center) as well as by the presence and concentration of quenching species within the primary coordination sphere of the emitting ion.[69] Because the direct excitation of lanthanide ions is inefficient due to the weak absorption of f–f transitions arising from low absorption cross-sections, indirect excitation *via* an appropriate chromophore represents an effective strategy.[70] In this process, the antenna absorbs UV-visible light and undergoes intersystem crossing from the singlet to the triplet excited state. Energy is then transferred intramolecularly from the antenna to the lanthanide ion, promoting its excitation through an energy transfer (ET) mechanism. The stored energy is subsequently released through radiative and/or nonradiative pathways, producing characteristic lanthanide luminescence before the ion relaxes back to its ground state. Notably, Tb^{3+} and Eu^{3+} display strong visible emissions, whereas Er^{3+}, Nd^{3+}, and Yb^{3+} primarily emit in the near-infrared region.[71] The properties of all lanthanide metals are summarized in Table 2.

The "antenna effect" refers to a mechanism in which an organic ligand functions as a light-harvesting antenna, efficiently absorbing optical energy and subsequently transferring it to a coordinated rare-earth ion through a molecular energy transfer pathway.[72,73] Typically, upon the absorption of excitation light at an appropriate wavelength, the ligand chromophore is promoted from the ground state (S_0) to the first excited singlet state (S_1). The excited molecule may then relax through either radiative or nonradiative processes. The transition from the singlet excited state (S_1) to the triplet excited state (T_1), known as intersystem crossing (ISC), plays a key role in this mechanism. Radiative relaxation results in molecular luminescence, which can occur as FL ($S_1 \rightarrow S_0$) or phosphorescence ($T_1 \rightarrow S_0$).[74]

In lanthanide-CD systems, carbon dots serve as sensitizers due to their abundant surface functional groups, enabling effective coordination with lanthanide ions. By strongly absorbing UV-visible light and transferring the harvested energy to the lanthanide centers, CDs act as sensitizers that enhance the lanthanide's luminescence. As a result, lanthanide ion-doped CDs often exhibit dual or multiple emission bands originating from both the CDs and lanthanide ions. Owing to this unique sensitization behavior, extensive research has been devoted to lanthanide ion-doped CDs and lanthanide-CD complexes for diverse applications. In this review, we comprehensively compile and organize, for the first time, reported studies on these systems and summarize their applications as fluorescent nanoprobes for the detection of a wide range of analytes.

3. Functionalization of CDs by lanthanide ions

Recently, most synthesized CDs exhibit relatively low emission efficiencies compared with conventional semiconductor quantum dots, even after surface passivation and/or functionalization. In many cases, additional passivation steps are necessary to achieve satisfactory luminescence, which complicates the synthesis process and restricts its scalability for large-scale applications. Consequently, developing effective strategies

to enhance the FL performance of CDs remains a significant challenge and is highly desirable to broaden their practical applications. In recent years, element doping has recently emerged as an effective strategy to tune the optical properties of CDs, producing highly luminescent materials and enhancing their electronic structure. Dopants are generally classified as metal atoms or heteroatoms (non-metal elements).[75,76]

Non-covalent surface modification serves as an effective approach for the surface functionalization of CDs with metal ions, enabling the introduction of new functionalities without substantially perturbing the core structure of the CDs. This approach is governed by non-covalent interactions, including electrostatic attraction, π–π stacking, and coordination (complexation), rather than covalent bonding. A key advantage of this method is the preservation of the CDs' core–shell architecture composed of sp^2-conjugated domains, with minimal impact on the surface electron cloud distribution.[77] Among these interactions, complexation is particularly important for metal-doped CDs, involving coordination between metal ions and surface functional groups such as amino, hydroxyl, and carboxyl moieties. Additionally, the complexation of amphiphilic molecules onto the CD surface enhances their solubility and stability in organic solvents through hydrophobic interactions. Overall, complexation enables effective tuning of CD surface properties, thereby extending their functional versatility and broadening their potential applications (Fig. 2).[45,78] For example, Liang *et al.* prepared Eu-CDs for the detection of ciprofloxacin and Ga^{3+}. Their work demonstrated that the interaction between Eu ions and CDs occurs through complexation, as confirmed by FTIR and XPS analyses, and their work further verified the successful formation of europium-doped CDs.[79] In addition, Yao *et al.* prepared novel lanthanide-doped CDs. Their results showed that Eu^{3+} can efficiently chelate with Cu-CDs, and the resulting Cu-CDs-Eu exhibits a larger average diameter than Cu-CDs, confirming the successful coordination between Cu-CDs and Eu^{3+}.[80]

The photoluminescence (PL) behavior of CDs is governed by multiple electronic transition pathways that are strongly influenced by their core structure, surface chemistry, and defect states. In undoped CDs, the intrinsic emission originates from $\pi \rightarrow \pi^*$ transitions within sp^2-hybridized carbon domains embedded in a sp^3 matrix, which typically results in size-dependent emission due to quantum confinement effects. In contrast, lanthanide ion-doped CDs (Ln-CDs) exhibit fundamentally different emission mechanisms dominated by the unique 4f electronic transitions of lanthanide ions. Upon doping, Ln^{3+} ions coordinate with oxygen- or nitrogen-containing surface groups of CDs, enabling ligand-to-metal charge transfer (LMCT) and efficient non-radiative energy transfer from the photoexcited CDs to the lanthanide centers *via* the antenna effect. The subsequent radiative relaxation of Ln^{3+} occurs through characteristic 4f–4f transitions, yielding narrow emission bands with long lifetimes and high color purity, as exemplified by the red emission of Eu^{3+} ($^5D_0 \rightarrow {}^7F_j$) and the green emission of Tb^{3+} ($^5D_4 \rightarrow {}^7F_j$). In some systems, the co-existence of CD-centered and lanthanide-centered emissions enables synergistic dual-emission behavior. The effect of CDs as sensitizers with lanthanide ions is shown in Fig. 3.

3.1 Types of doping

Doping is a widely used strategy to improve the physicochemical properties of CDs, with heteroatom doping and surface functionalization being among the most effective approaches for tuning their optical, electrical, and chemical characteristics.

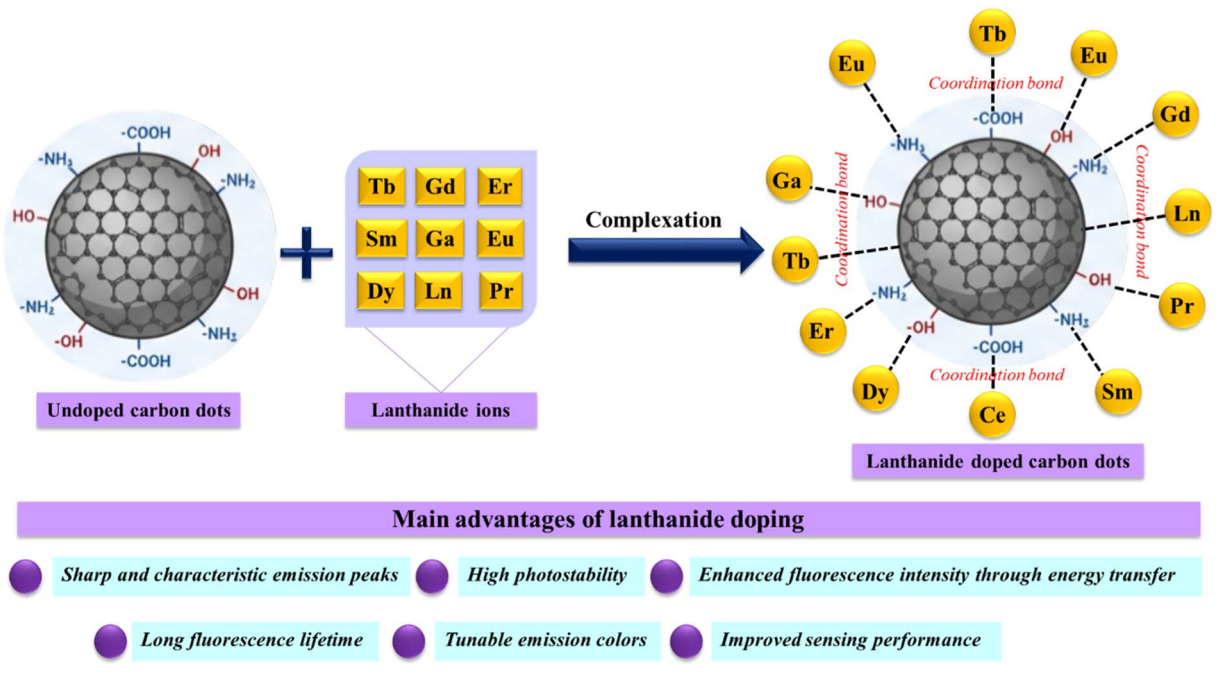

Fig. 2 Schematic of the complexation of CDs with lanthanide ions.

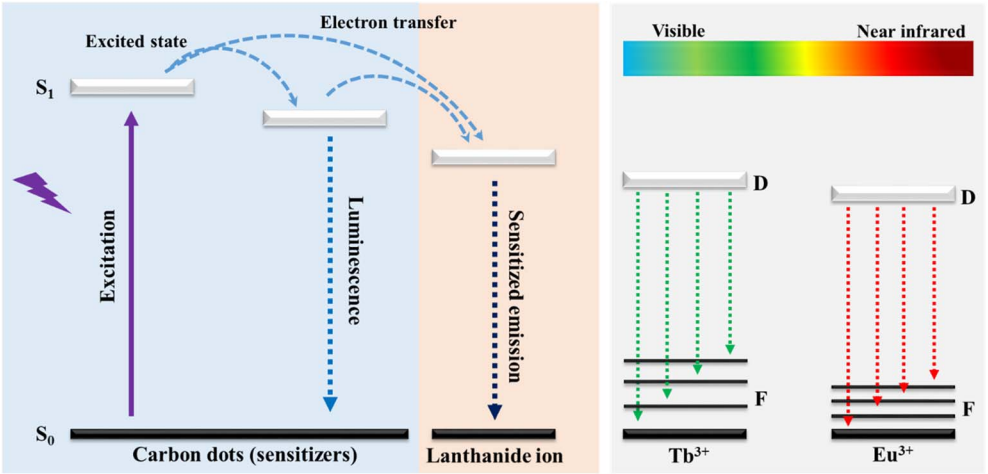

Fig. 3 Schematic of CDs as sensitizers with lanthanide ions.

In heteroatom doping, non-metal atoms such as nitrogen, boron, sulfur, and phosphorus are introduced into the carbon framework, which modifies the electronic structure of CDs and generates n-type or p-type charge carriers. As a result, the optical and electronic properties of CDs can be precisely controlled by adjusting the type and concentration of dopant atoms.[59] Metal-ion doping represents another important approach to enhance the functionality of CDs. Transition and rare-earth metal ions, including Fe^{3+}, Ni^{2+}, Cu^{2+}, and Mn^{2+}, possess partially filled d- or f-orbitals and numerous unoccupied orbitals that can interact with the carbon matrix. Their incorporation introduces localized electronic states within the band structure and disrupts the intrinsic sp^2-conjugated π-system, thereby modulating the energy bandgap and facilitating new electronic transitions and charge transfer processes. Consequently, properties such as optical absorption, electrical conductivity, PL, and even magnetic behavior can be significantly improved.[45] In addition, halogen doping has been shown to enhance the quantum yield and photophysical properties of CDs. For instance, fluorine, which has the highest electronegativity among all elements, can strongly attract neighboring electrons, promoting charge separation and improving luminescence efficiency. Fluorine edge doping can also replace hydrogen atoms in conjugated organic structures while preserving the sp^2-hybridized π-conjugated system of the carbon core.[81,82] Furthermore, lanthanide doping provides unique optical advantages due to the characteristic 4f–4f electronic transitions of rare-earth ions such as Eu^{3+} and Tb^{3+}. When incorporated into CDs, these ions act as luminescent centers and receive excitation energy from the carbon matrix through energy transfer processes. This dual effect, involving both electronic structure modification and energy transfer, enables the precise tuning of emission wavelengths, overall sensing performance of CDs, and quantum yields.[83] In Table 3, the different types of doping and their effects on the characteristics of CDs are summarized.

4. Optical properties of carbon dots

4.1 UV-vis absorbance of CDs

CDs typically exhibit strong absorption in the ultraviolet region, along with a broad tail extending into the visible range. Most absorption bands are commonly observed between 260 and 350 nm. The prominent absorption peak around 230 nm is mainly associated with the π–π* electronic transitions of aromatic C=C bonds.[84] The shoulder peak near 300 nm is assigned to n–π transitions arising from surface functional groups, such as C=O

Table 3 Summary of typical dopants in CDs and their effects on optical and structural properties

Doping type	Examples	Key effect on carbon dots
Heteroatom doping	N, S, P, B	Modifies the electronic structure, generates n- or p-type carriers, and enhances the photoluminescence and quantum yield
Metal-ion doping	Fe^{3+}, Ni^{2+}, Cu^{2+}, Mn^{2+}	Introduces localized electronic states, alters the HOMO–LUMO gap, and improves charge transfer and sensing performance
Halogen doping	F, Cl, Br	Alters the electron distribution due to high electronegativity and increases the quantum yield and photophysical stability
Lanthanide doping	Eu^{3+}, Tb^{3+}, Sm^{3+}, Gd^{3+}	Provides characteristic 4f–4f luminescence, enabling tunable emission and improved fluorescence sensing

bonds[85] as well as other heteroatom-containing groups, including nitrogen and oxygen.[86]

4.2 Fluorescence of CDs

FL is considered one of the most remarkable properties of CDs. CDs synthesized through various methods and precursor materials often exhibit different chemical compositions and structural features. Generally, the FL emission of CDs can originate from several factors, including the quantum size effect, surface states, and molecular states.[87] However, the precise mechanism responsible for the FL behavior of CDs is still debated and requires further investigation.[88] Among the proposed mechanisms, the quantum confinement effect, also known as the size effect, is one of the most widely accepted models used to explain the FL properties of CDs.[89,90] Typically, the bandgap energy of CDs is influenced by their particle size and morphology. In recent years, increasing attention has been directed toward studying the role of quantum size effects in CDs.[91]

4.3 Quantum yield (QY)

CDs exhibit notable optical properties, among which the QY is a key parameter that reflects their efficiency in converting absorbed photons into emitted light. This value represents the ratio of emitted photons to absorbed photons and is commonly used to evaluate the efficiency of the PL process.[92] CDs with high QYs are particularly desirable for various applications, especially FL imaging and sensing, where a strong and stable emission is essential for precise detection and visualization.[93] The QY of carbon dots is influenced by several factors, including synthesis methods, surface functionalization, chemical composition, and particle size distribution.[94] Tian *et al.* used folic acid and terbium nitrate as precursors to prepare CDs, Tb-CDs, and Tb@CDs. The QYs of the prepared CDs, Tb@CDs, and Tb-CDs were calculated to be 57.12%, 48.2%, and 73.8%, respectively.[95] Wu *et al.* developed novel lanthanide-doped CDs. The probe was prepared from citric acid, ethylenediamine, and lanthanide ions using a hydrothermal method. The obtained CDs exhibited excitation-dependent FL behavior. The FL quantum yields of Yb-CDs and Nd-CDs at 360 nm were calculated to be 52.32% and 49.06%, respectively.[96]

4.4 Lifetime measurement

The fluorophore lifetime refers to the average duration that a molecule remains in the excited state before returning to the ground state.[97] The FL lifetime is considered an intrinsic property of fluorescent materials. CDs that exhibit relatively long FL lifetimes may have promising applications in sensing and imaging. However, the FL lifetime of CDs is typically only a few nanoseconds.[98] In sensing studies, a decrease in FL lifetime after the addition of an analyte generally suggests a dynamic quenching mechanism. In contrast, if the lifetime remains unchanged while the FL intensity decreases, the quenching process is often attributed to the inner filter effect (IFE) or static quenching, as reported in several studies.[99,100] For example, Meng *et al.* prepared Eu-CDs for the detection of tetracycline (TC). The sensing mechanism was investigated using FL lifetime measurements. The fluorescence lifetimes of Eu-CDs were measured to be 5.13 ns in the absence of TC and 4.92 ns in the presence of TC, indicating that the addition of TC caused only a negligible change in the FL lifetime. These results suggest that energy transfer between the CDs and TC is minimal, and the decrease in the blue FL emission intensity of the CDs can be attributed to the IFE rather than dynamic quenching.[101] Similarly, Yan *et al.* demonstrated that the sensing mechanism for caffeic acid detection was also based on the IFE mechanism. Their fluorescence lifetime measurements showed that the FL lifetime remained almost unchanged before and after the addition of caffeic acid, further confirming that the observed FL quenching was mainly caused by the IFE.[102]

5. Sensing mechanisms

Several mechanisms can explain FL quenching and sensing behavior in CD systems, including the IFE, Förster resonance energy transfer (FRET), photo-induced electron transfer (PET), and static or dynamic quenching processes. The inner filter effect occurs when the absorption of excitation or emitted light reduces the observed FL intensity, leading to fewer emission signals; this attenuation may arise from the primary absorption of the excitation light or the secondary absorption of the emitted FL. Unlike energy transfer mechanisms, the FL lifetime in IFE-based quenching generally remains unchanged, which allows it to be distinguished from other processes.[103] In contrast, FRET involves non-radiative energy transfer from an excited donor to an acceptor through long-range dipole–dipole interactions, often requiring spectral overlap between the donor emission and acceptor absorption as well as an appropriate intermolecular distance. In CD-based sensors, CDs commonly act as energy donors, and FRET can either reduce the FL intensity or cause emission wavelength shifts, depending on the interaction with the target or quencher.[104] PET is another quenching mechanism in which electron transfer occurs between the excited fluorophore and an electron donor or acceptor analyte, forming a transient complex that relaxes to the ground state without photon emission.[105] Additionally, FL quenching can be categorized into static and dynamic processes: static quenching arises from the formation of a non-fluorescent ground-state complex between the fluorophore and quencher without altering the FL lifetime, whereas dynamic quenching occurs through collisional interactions in the excited state, typically resulting in a reduced FL lifetime while leaving the absorption spectrum largely unchanged.[32]

6. Applications of lanthanide ion-doped carbon dots

6.1 Metal-ion detection

Metal ions are widely distributed in the natural environment, and their detection is essential for environmental and biomedical applications. Variations in the concentrations of specific metal ions can indicate pathological conditions in the body, offering potential tools for early diagnosis and disease monitoring.[106–108]

Xu *et al.* developed an Eu-CDs/MOF-based sensor for Hg^{2+} detection, exhibiting a wide linear working range of 0.065–150 μM and a limit of detection (LOD) of 13 ppb.[109] Sang *et al.*[110] reported Eu-CDs for the dual sensing of TC and Al^{3+}. Upon increasing the TC concentration, the FL emission color of the Eu-CDs progressively shifted from blue to light purple and finally to red. The FL intensity ratio showed a good linear correlation in the concentration range of 0–100 μM, with a LOD of 6.9 nM. Conversely, the subsequent introduction of Al^{3+} at different concentrations induced a reverse color transition from red to pink and ultimately back to blue. A linear correlation was observed between the FL intensity and Al^{3+} concentration in the working range of 0–50 μM, with a LOD of 28.6 nM. In addition, a smartphone-based visual assay platform was developed, achieving visual detection limits as low as 13.2 nM for TC and 160 nM for Al^{3+}, as illustrated in Fig. 4.

Desai *et al.* fabricated a fluorescent nanosensor based on Eu^{3+}-CDs. The addition of Hg^{2+} ions led to significant quenching of the Eu^{3+}-CD FL emission, and a linear correlation between the FL quenching intensity and Hg^{2+} concentration was observed in the working range of 5.0–250 μM, with a LOD of 2.2 μM.[111] Similarly, Correia *et al.* synthesized Eu-CDs and demonstrated that their luminescence was selectively quenched by Hg^{2+} and Ag^{+} ions, while remaining largely unaffected by other metal cations. Notably, the quenching mechanism depended on the specific ion: both the blue emission of the carbon dots and the red emission of Eu^{3+} were suppressed in the presence of Hg^{2+}, whereas only the carbon dot emission was quenched by Ag^{+}. Based on these distinct responses, a ratiometric sensing strategy was established using the intensity ratio of carbon dot emission to Eu^{3+} emission. Eu-doped carbon dots show higher sensitivity to metal cations than undoped CDs due to structural changes caused by the incorporation of Eu ions. These ions coordinate with functional groups during synthesis, act as nucleation centers, and modify the carbon network structure. As a result, additional defects and active sites are formed, enhancing the interaction of Eu-CDs with metal cations and improving their sensing performance. The limits of detection were approximately 5 μM for Ag^{+} and 4 μM for Hg^{2+}, with an effective working concentration range of 10–100 μM.[112]

Other lanthanide ion-doped carbon dots (CDs), such as Ce-doped CDs, have also been reported. For example, Zhang *et al.* used Ce-doped CDs for the determination of As(III), achieving a working range of 0.5–5.8 μg L^{-1} and a LOD of 0.2 μg L^{-1}.[113] Another example is the work by Mohandoss *et al.*, who developed a sensor for the dual detection of Fe^{3+} and pyrophosphate (PPi) ions. The sensor exhibited high sensitivity, with LODs of 34.6 nM for Fe^{3+} and 25.4 nM for PPi.[114] Chai *et al.* reported a Dy-CD system in which Dy^{3+} ions induced the aggregation of CDs. In the presence of phosphate (PO_4^{3-}), strong Dy^{3+}-phosphate coordination disrupted these aggregates, resulting in FL recovery of the CDs. This mechanism enabled the selective detection of PO_4^{3-} in artificial wetland samples, with a working range of 0.2–30 μM and a LOD of 0.1 μM.[115] In another study, Kumar *et al.* developed Er-CDs with an enhanced quantum yield, which were employed as a FL probe for the turn-off/turn-on sensing of Fe^{2+} ions and H_2O_2. The FL of Er-CDs was quenched upon the addition of Fe^{2+} and subsequently restored after introducing H_2O_2, achieving detection limits of 51.7 nM for Fe^{2+} and 55 μM for H_2O_2.[83] More research on metal-ion detection using Ln-CDs is summarized in Table 4.

6.2 Pharmaceutical detection

In pharmaceutical applications, analytical chemistry plays a crucial role in the identification and quantification of active compounds, evaluation of their purity and stability, and assurance of pharmaceutical product quality throughout manufacturing and storage.[126]

Li *et al.* developed a ratiometric fluorescent probe to detect TC, achieving a LOD of 31 nM and a working range of 1–100

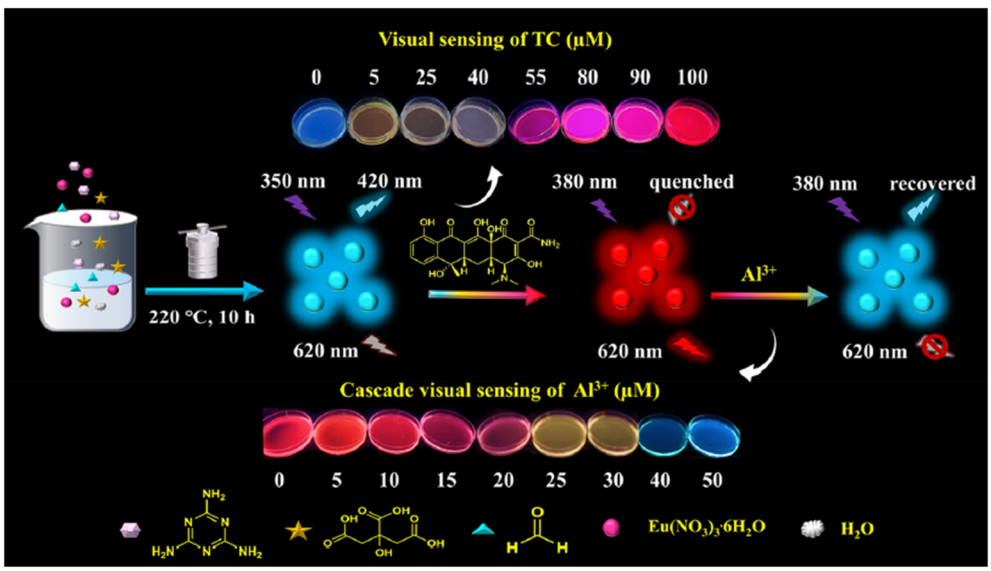

Fig. 4 Schematic of Eu-CD synthesis and colorimetric sensing for TC and Al^{3+}, reproduced with permission from ref. 110. Copyright 2022, Elsevier.

Table 4 An overview of Ln-CDs as fluorescent nanoprobes for multiple metal ions, highlighting their analytical features and merits

Types of Ln-CDs	Analyte	Sample	LOD (nM)	Working range	Ref.
Gd-CDs	Hg^{2+}	Water	104.4, 60.2	0–50 μM	116
Gd-CDs	Cu^{2+}	Water	380	0–38.4 μM	117
Ln-CDs	Hg^{2+}	Cancer cells	100	0 mM–50 μM	118
Ln-CDs	Fe^{3+}, Sn^{2+}, ClO^-	Zebrafish	990, 110, 110	0–100 μM	119
Ln-CDs	Fe^{3+}	HeLa cells	91	0.15–10.0 μM	120
Eu/Tb-CD	Cr(VI)	—	175	1–20 μM	121
Eu/Tb-CDs	Ag^+ and Hg^{2+}	Water	50.1, 33.3	0–10 μM	122
La/Ce-CDs	Fe^{3+}	Water	753	0–60 μM	123
Pr-CDs	Hg^{2+}	Water	90.3	0–10 μM	124
Tb-CDs	Hg^{2+}	Seafood	37	1–161.51 μM	125

μM.[127] Similarly, Liang *et al.*[79] developed a novel probe based on Eu-CDs for the detection of ciprofloxacin (CIP) and gallium ions (Ga^{3+}). In addition to fluorescence sensing, a hydrogel-based sensing chip was fabricated, with a smartphone employed as the detector. Under irradiation with a 360-nm ultraviolet lamp, the emission of the chip containing increasing concentrations of CIP gradually changed from negligible fluorescence to bright red. Within the concentration range of 5.0–200.0 μM, the CIE-R value of the chip showed a linear correlation with the CIP concentration. After the addition of Ga^{3+} (0.5–70.0 μM) to the chip pretreated with 215 μM CIP, the FL color gradually changed from bright red to bright blue.

Wu *et al.* reported a novel probe for oxytetracycline (OTC) and tetracycline (TC) detection based on Eu-CDs. In this system, Eu^{3+} ions chelated with CDs and specifically recognized OTC and TC. Owing to the dual and reverse FL responses, the ratiometric detection of OTC and TC was achieved in the working ranges of 0.1–45 μM and 0.1–30 μM, with detection limits of 17 nM and 41 nM, respectively. In addition, a smartphone-assisted portable device was developed for OTC detection. As shown in Fig. 5, the probe was prepared in 24-well plates, and upon the addition of OTC, a gradual change in the FL color was observed. FL images were captured using a smartphone camera and converted into RGB values. With increasing OTC concentration, the *R* value increased, accompanied by a decrease in the *B* value.[100]

Liu *et al.* also developed an Eu-CD-based sensor for TC detection. The sensor enabled rapid and sensitive TC detection using both FL and colorimetric methods, with LODs as low as 2.82 nM and 3.74 nM, respectively.[128] Ma *et al.* developed a ratiometric fluorescent probe based on Eu-CDs for the detection of TC. The proposed sensor exhibited a wide working range of 0.05–45 μM and a low LOD of 5.92 nM for TC.[129] In addition, Hu *et al.*[130] designed a multiple-response fluorescent

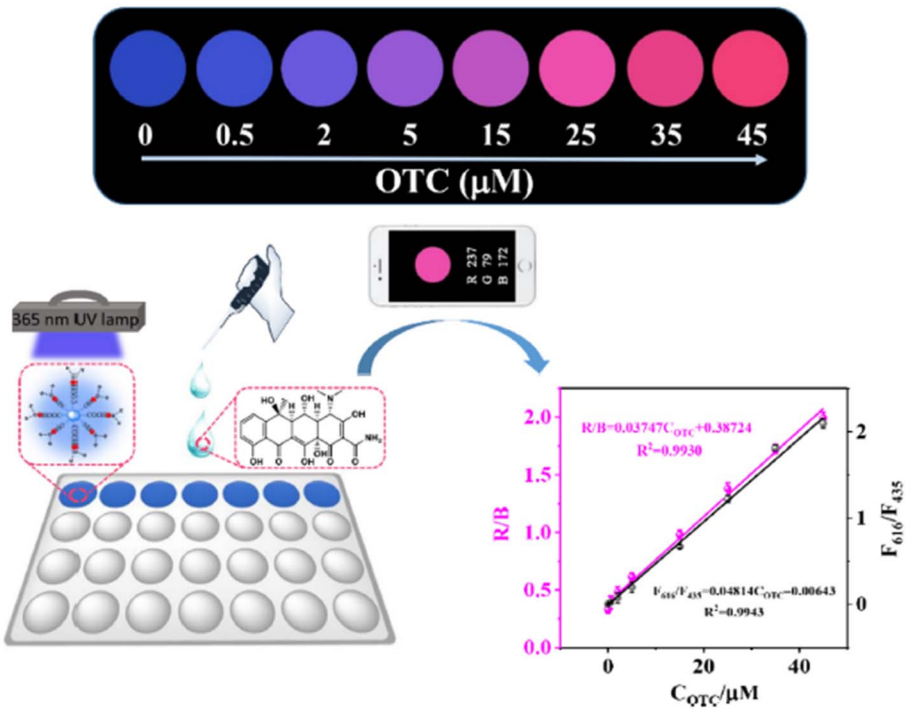

Fig. 5 Smartphone-based platform for the quantitative detection of OTC, reproduced with permission from ref. 100. Copyright 2023, Elsevier.

probe composed of dual-emission Eu-CDs for the determination and discrimination of TCs. The carboxyl and amino groups on the dual-emission carbon dots coordinated with Eu^{3+} to form the Eu-CD complex. Upon the addition of TCs, the FL intensities of CDs were quenched due to the IFE and localized FL resonance energy transfer between Eu-CDs and TCs. Simultaneously, the chelation between Eu-CDs and TCs enhanced the antenna effect, resulting in increased characteristic Eu^{3+} emission peaks. Based on these responses, TCs were detected with low detection limits ranging from 46.7 to 72.0 nM. In addition, discrimination among different TCs was achieved through variations in the L-FRET efficiency. Furthermore, a novel centrifuged lateral flow assay strip (CLFAS) device was developed by integrating Eu-CDs, lateral flow assay strips, and a smartphone, enabling TC detection through RGB value variations, as illustrated in Fig. 6.

More research on pharmaceutical product detection using Ln-CDs is summarized in Table 5.

6.3 Contaminant detection

Rapid population increase and industrialization have intensified environmental pollution, endangering ecosystems and human health through contaminants such as dyes, mycotoxins, organic compounds, and pathogens.

Abdel-Lateef *et al.* developed Eu-CDs for the detection of curcumin adulteration by metanil yellow. The probe was synthesized through the carbonization and conversion of a tannic acid–Eu complex into highly fluorescent Eu-CDs. The proposed method exhibited a LOD of 1.05 nM with a linear detection range of 1.0–15.0 μg mL^{-1}.[154] Similarly, Zhang *et al.* designed a novel probe for ATP detection by simply mixing CDs with calcein-Eu. In this system, the carbon dots served as the internal reference, while calcein-Eu acted as the recognition unit. The probe showed a dynamic linear range of 0.05–2.0 μM, with a LOD of 20 nM.[155] Furthermore, Zhang *et al.* developed a sensor based on Eu-CDs. The sensor exhibited a broad working range (0–2.5 μM), an extremely low LOD (1.25 nM), and a rapid response time (<40 s). Furthermore, a smartphone-based method enabled the portable, visual quantification of Fe^{3+} with a practical LOD of 6.588 nM.[156] In addition, Qin *et al.* prepared a novel ratiometric probe for the biomarker diaminotoluene using a Eu-CD-encapsulated MOF, achieving a LOD of 6.8 μg mL^{-1}.[157]

Amin *et al.* developed Eu-CDs for the determination of selenite. The method had a simple procedure that enabled the selective detection of selenite, with a working range of 0.078–21.4 μg mL^{-1} and a LOD of 53.0 ng mL^{-1}.[158] Similarly, Zhou *et al.* prepared CDs doped with Eu *via* direct coordination for the detection of UO_2^{2+} within the working range of 25–200 nM,

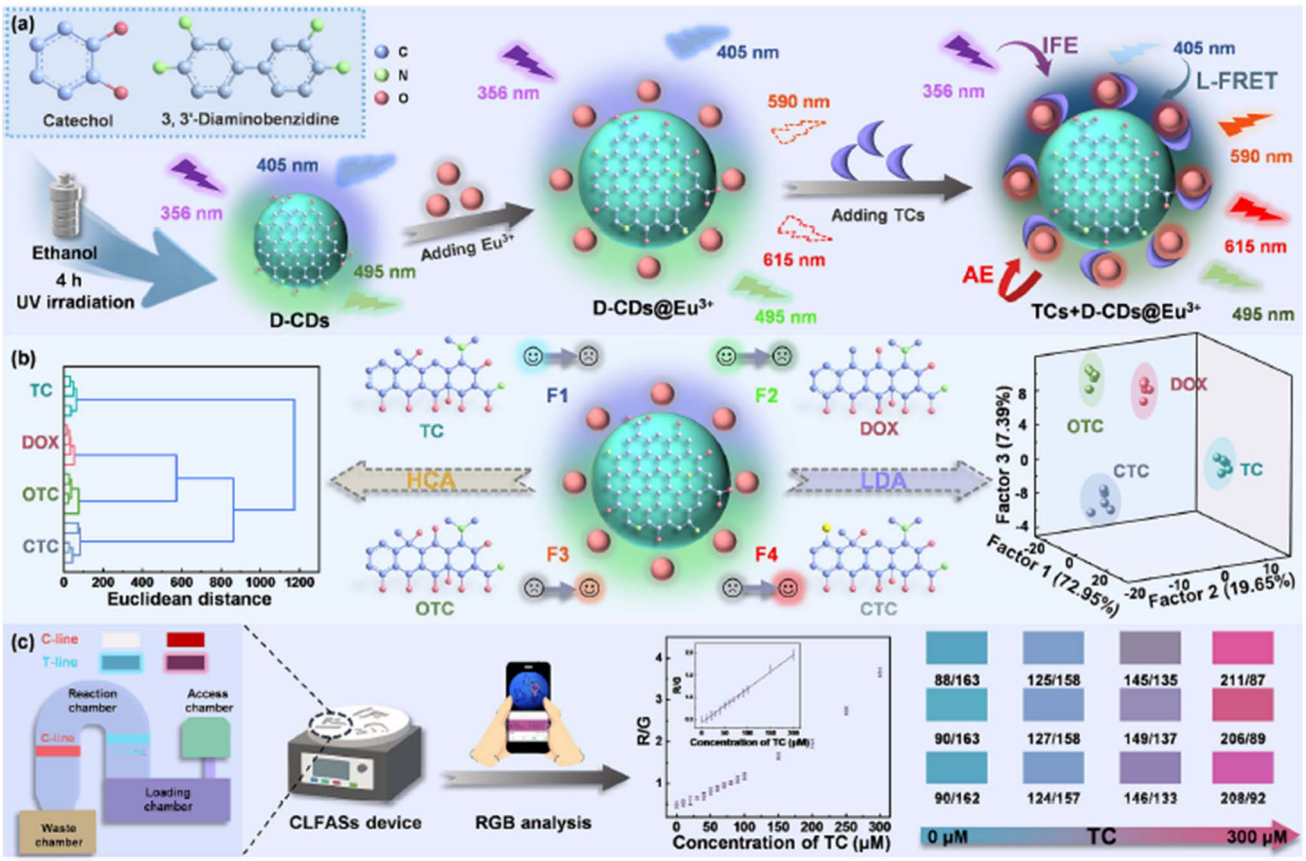

Fig. 6 Schematic representation of (a) the Eu-CD probes, (b) discrimination among four TCs, and (c) the CLFAS device, reproduced with permission from ref. 130. Copyright 2024, Elsevier.

Table 5 An overview of Ln-CDs as fluorescent nanoprobes for multiple pharmaceuticals, highlighting their analytical features and merits

Types of Ln-CDs	Analyte	Sample	LOD (nM)	Working range	Ref.
Eu-CDs	TC	Milk, honey, water	36.1	0.4–60 μM	80
Eu-CDs	TC	Water	5.8	0.01–3 μM	131
Eu-CDs	OTC, TC, DC, CTC	Chicken, pork, fish	9.50, 15.80, 10.40, 90.30	0.00–603.75 μM, 0.00–623.82 μM, 0.00–594.61 μM, 0.00–601.54 μM	132
Eu-CDs	TC	Water, milk, honey, serum	3	0–80 μmol L^{-1}	133
Eu-CDs	TC	Water, milk	3.83	0.01–240 μM	134
Eu-CDs	TC	Milk, water	7.9	25–2000 nM	135
Eu-CDs	TC	Water	12	0.08–5 μM	136
Eu-CDs	TC	Milk, honey, water	8.7	25 nM to 20 μM	137
Eu-CDs	OTC	Honey, milk	150	0–100 μM	138
Eu-CDs	TC	Milk, water	22.6	0.1–50 μM	139
Eu-CDs	TC	Water, milk	8.2	0–20 μM	140
Eu-CDs	TC	—	11.7	0–3.5 μg mL^{-1}	141
Eu-CDs	OTC	Water, milk	29	0.1–25 μM	142
Eu-CDs	TC, OTC	Water	2.96, 2.85	0.0067–25 μM, 0.0067–21 μM	143
Eu-CDs	TC, OTC	Bovine, goat, milk	29, 16	0.25–20 μM, 20–70 μM	144
Eu-CDs	TC	Water	30	0.1–100 μM	145
Eu-CDs	OTC	Water	9.6	0–10 μM	146
Eu-CDs	TC	Water	2.7	0.04–2.4 μM	147
Ln-CDs	OTC, TC	Pork, fish	42.90, 83.30	0.00–805.20 μM, 0.00–1039.50 μM	148
Tb-CDs	Fluoroquinolones	Milk	9.1	0.5–58 μM	149
Tb-CDs	Ciprofloxacin	Milk, urine	1.6	0.008–120 μM	150
Tb-CDs	Alogliptin	Water, plasma	88.09	0.01–1.5 μg mL^{-1}	151
Tb-CDs	Edoxaban	Human plasma	11.04	30.0–350.0 ng mL^{-1}	152
Tb-CDs	Deferasirox	Serum	80	0.1–2.5 μM	153

achieving a LOD of 0.84 nM (0.42 μg L^{-1}).[159] Lastly, Albalawi *et al.* prepared Eu-doped CDs for the detection of indigo carmine dye over the working range of 1.5–10.0 μg mL^{-1}, with a LOD of 0.40 μg mL^{-1}.[160]

More research on contaminant detection using Ln-CDs is summarized in Table 6.

6.4 Anthrax biomarker detection

Anthrax is a zoonotic infectious disease caused by *Bacillus anthracis*.[164] Individuals who inhale more than 10^4 *Bacillus anthracis* spores at a single exposure and fail to receive effective treatment within 48 h face a high risk of mortality.[165] As an emerging class of biological contaminants, anthrax spores pose an extreme threat not only to animals and plants but also to humans. Among their components, 2,6-pyridinedicarboxylic acid (DPA) is a key constituent and serves as a major biomarker of anthrax spores.[166] Even at low levels (around 60 μM), *Bacillus anthracis* spores can severely harm human health and are associated with a high fatality rate.[167]

Li *et al.* reported the preparation of a europium-containing CD probe for the detection of DPA and copper ions. In this system, the red emission originating from Eu^{3+} increased with increasing DPA concentration, whereas it decreased after the addition of Cu^{2+}. Subsequently, the introduction of glutathione (GSH) restored the red emission. Therefore, the probe operated based on an "on–off–on" sensing mechanism. The corresponding LODs were determined to be 137 nM for DPA, 80 nM for Cu^{2+}, and 50 nM for GSH, respectively.[55] Similarly, Song *et al.* developed a ratiometric probe based on Eu/CDs/guanosine monophosphate disodium (GMP) for the detection of DPA. In this system, the CDs served as the reference signal, while Eu^{3+} acted as the analytical signal. The FL intensity of Eu^{3+} increased with increasing DPA concentration. The probe exhibited a LOD of 5.1 nM and a linear working range from 15 nM to 5 μM.[168] Additionally, Zhou *et al.* developed another Eu-CD-based ratiometric probe for DPA detection using both colorimetric and visual assays. The LOD for the ratiometric colorimetric assay was 10.6 nM. More notably, naked-eye detection of DPA without instrumental assistance was achieved at concentrations as low as 1.0 μM.[169] Lastly, Du *et al.*[170] developed Eu-CDs *via* complexation for the detection of the DPA biomarker. The probe was successfully applied in two modes: ratiometric

Table 6 An overview of Ln-CDs as fluorescent nanoprobes for multiple contaminants, highlighting their analytical features and merits

Types of Ln-CDs	Analyte	Sample	LOD (nM)	Working range	Ref.
Tb-CDs	Phosphates (Pi)	Frozen seafoods	410	0.5–12 μM	161
Tb-CDs	2,4,6-Trinitrophenol	Water	200	500 nM–100 μM	162
Tb-CDs	Melamine	Milk, infant formula	2.6	0.01–300 μM	163

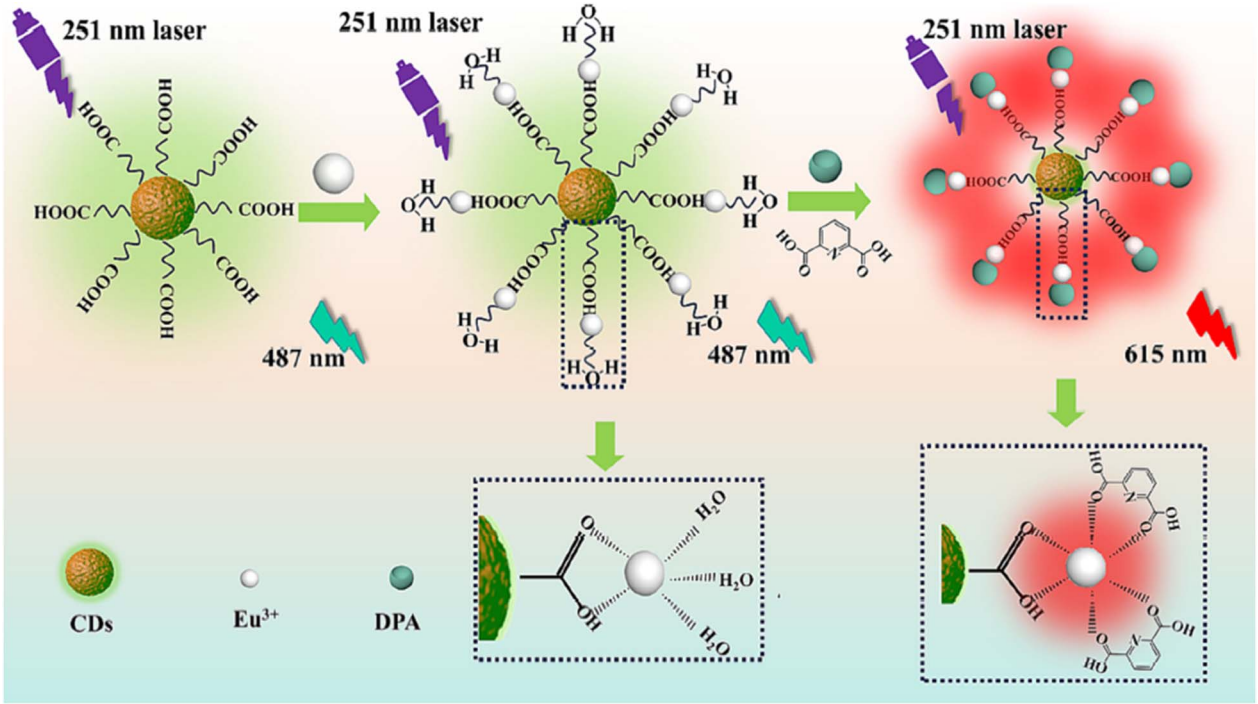

Fig. 7 Schematic of DPA detection based on Eu-CDs, reproduced with permission from ref. 170. Copyright 2025, Elsevier.

sensing and paper-based sensing. The ratiometric method exhibited a working range of 0–120 μM with a LOD of 7.566 nM, while the paper-based method showed a working range of 0–100 μM, as depicted in Fig. 7.

More research on anthrax biomarker detection using Ln-CDs is summarized in Table 7.

6.5 Biomolecule detection

Biomolecules are essential to physiological functions and are intimately linked to the initiation and progression of numerous diseases. Consequently, developing analytical methods that are efficient, sensitive, rapid, selective, and cost-effective for biomolecule detection is of great significance.[178]

GSH plays a vital role in biological systems and performs diverse cellular functions. Al-Mashriqi *et al.* prepared Eu-CDs as nanoprobes for the detection of GSH, which exhibited a high quantum yield of 40.67%. The LOD was 30 nM, and the linear working range was 0–50 μM.[24] Similarly, Liu *et al.* developed a new ratiometric FL probe based on Eu-CDs for the detection of cerebrospinal Aβ monomers, with a linear range of 0.5–100 nM and a LOD of 0.17 nM. The probe was successfully applied to rat samples.[179] Furthermore, Li *et al.* prepared Eu-CDs for the detection of Fe^{3+} and ascorbic acid based on an 'off–on' FL strategy. The FL intensity ratio of the Eu-CDs showed an excellent linear relationship with the concentrations of Fe^{3+} and ascorbic acid, with limits of detection of 0.15 and 0.13 μM, respectively. The method was successfully applied to water and food samples.[180] Lastly, Li *et al.*[181] reported an effective synthesis strategy for imidazole-based ionic liquid-functionalized carbon dot hybrids (APM-CDs). Using these materials, a novel photofunctional hybrid probe, Eu-CDs, was fabricated. The FL intensity of Eu-CDs exhibited a strong linear correlation with the ascorbic acid concentration in the range of 25–500 μM, achieving a LOD of 80 nM, as illustrated in Fig. 8.

Tian *et al.* prepared a ratiometric FL probe for ascorbic acid based on Eu-CDs. A wide linear detection range from 0.5 to 820

Table 7 An overview of Ln-CDs as fluorescent nanoprobes for multiple anthrax biomarkers, highlighting their analytical features and merits

Types of Ln-CDs	Analyte	Sample	LOD (nM)	Working range	Ref.
Eu-CDs	DPA	Water, FBS, soil	5	5–700 nM	171
Eu-CDs	DPA	Water, bacteria	23	0.1–100 μM	172
Tb-CDs	DPA	Water	44	0.05–8 μM	95
Tb-CDs	DPA	—	5	0.005–1.2 μM	173
Tb-CDs	DPA	Orange juice, water	0.1	0.0005–2.5 μM	174
Tb-CDs	DPA	Spinach, cucumber, pear	3.0	0–0.091 mM	175
Tb-CDs	DPA	Rice	680	0–20 μM	176
Tb-CDs	DPA	—	5	0.005–1.2 μM	173
Tb-CDs	DPA	Water	35.9	0.5–6 μM	177

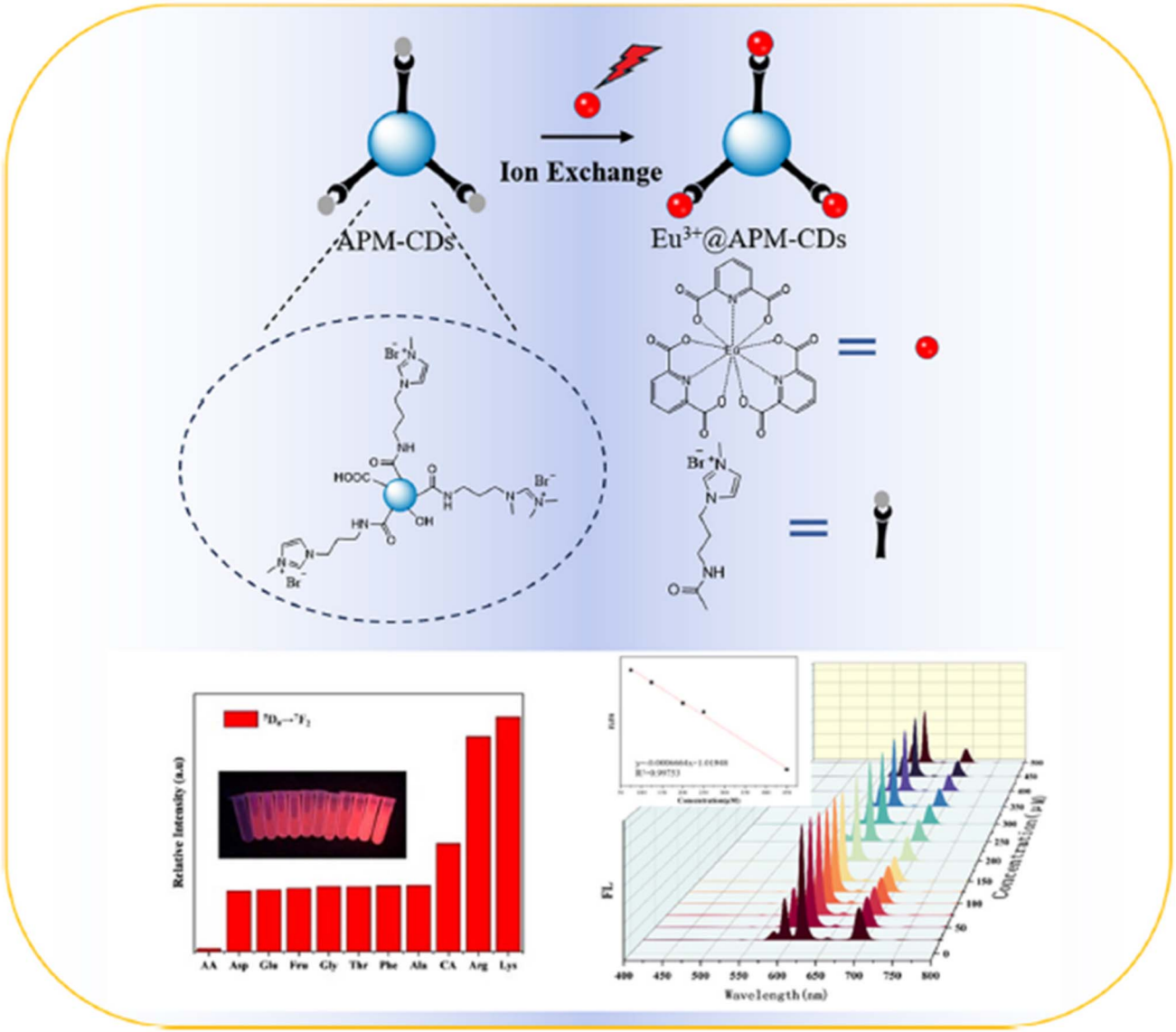

Fig. 8 Schematic of ascorbic acid detection using Eu-CDs, reproduced with permission from ref. 181. Copyright 2024, Elsevier.

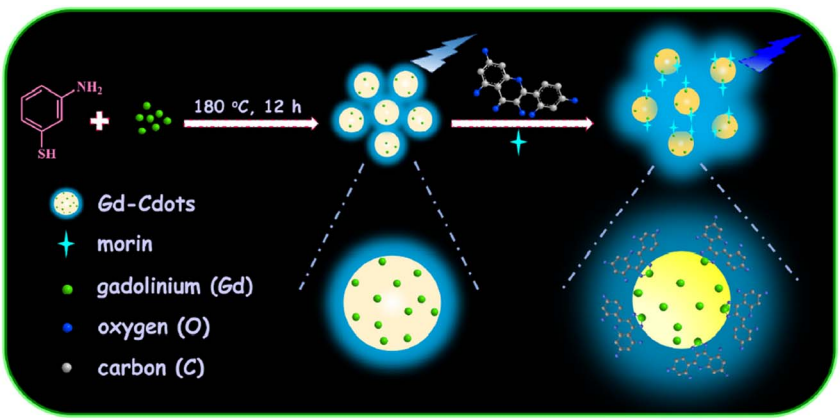

Fig. 9 Schematic of the Gd-CD preparation and applications, reproduced with permission from ref. 183. Copyright 2022, Elsevier.

Table 8 An overview of Ln-CDs as fluorescent nanoprobes for multiple biomolecules, highlighting their analytical features and merits

Types of Ln-CDs	Analyte	Sample	LOD (nM)	Working range	Ref.
Gd-CDs	Dopamine hydrochloride (DH)	Human urine, mouse serum	1.26	1–10 μM	184
Ln-CDs	Serotonin	Urine	7.4	0–38 nM	185
Sm-CDs	Epinephrine	Urine	28.1	0–105 nM	186
Tb-CDs	Bovine serum albumin	Bovine serum	42	0.1–650 μM	187
Tb-CDs	5-Hydroxytryptamine, 5-hydroxyindole-3-acetic acid	Artificial blood Plasma, synthetic urine	0.44, 0.49	$0.0–2.60 \times 10^{-7}$ M, $0.0–2.91 \times 10^{-7}$ M	188
Tb-CDs	H_2O_2	Rat serum	60	0–40 μM	189
Tb-CDs	Adenosine 5′-triphosphate	Human serum	8.5	40 nM-4.0 μM	190
Tb-CDs	Cytochrome c	Human serum	0.35	1–50 nM	191
Tb-CDs	Guanosine 3′-diphosphate-5′-diphosphate (ppGpp)	Serum, urine	50	0.5–15 μM	192
Tb-CDs	DNA	Synthetic samples	0.80	80 ng mL^{-1}–50 μg mL^{-1}	193

μM was achieved, with a LOD of 60 nM.[182] In addition, Wang *et al.* developed a ratiometric probe based on Gd-CDs for the determination of morin in biological samples. Owing to the specific chelation between Gd^{3+} and morin, a ratiometric FL nanosensor was constructed, which exhibited a linear detection range of 0.04–80.0 μM and a LOD of 25.0 nM. In addition, the color of the Gd-CDs changed from colorless to deep yellow upon interaction with morin, enabling the development of a colorimetric nanosensor. This method showed two working ranges of 0.04–15.0 μM and 15.0–93.0 μM, with corresponding LODs of 10.5 nM and 21.2 nM, respectively,[183] as illustrated in Fig. 9.

More research on biomolecule detection using Ln-CDs is summarized in Table 8.

7. Conclusion and future perspectives

Fluorescent nanomaterials have seen rapid development as sensing probes in recent years owing to their unique optical and physicochemical characteristics, along with their high sensitivity, selectivity, targeting capability, and strong suitability for detection applications. Researchers are increasingly focused on developing analyte nanosensors that combine high selectivity and sensitivity, as such systems that offer cost-effective solutions for environmental and analytical monitoring, and this review highlights the significant role of Ln-CDs in this context. Owing to their simple and economical synthesis and strong reactivity toward a broad range of targets, Ln-CDs represent promising platforms for the detection of diverse analytes, including metal ions, pharmaceuticals, contaminants, anthrax biomarkers, and biomolecules, often achieving nanomolar level detection limits that reflect their high analytical performance.

Although Ln-CDs are promising platforms and they are widely used for the detection of various analytes, several challenges remain, including the need for a deeper understanding of lanthanide doping mechanisms and their influence on the electronic structure and photophysical properties of carbon dots, the development of scalable and environmentally friendly synthesis strategies, the expansion of multianalyte sensing capabilities for complex sample matrices, and the integration of Ln-CDs into portable or wearable sensing devices. Sustained interdisciplinary advances will likely make Ln-CDs vital to upcoming smart and sustainable analytical technologies.

Conflicts of interest

There are no conflicts to declare.

Data availability

Data sharing is not applicable to this article, as no datasets were generated or analysed during the current study.

References

1 M. Nadporozhskaya, N. Kovsh, R. Paolesse and L. Lvova, Recent advances in chemical sensors for soil analysis: a review, *Chemosensors*, 2022, **10**(1), 35.
2 T. Arakawa, D. V. Dao and K. Mitsubayashi, Biosensors and chemical sensors for healthcare monitoring: a review, *IEEJ Trans. Electr. Electron. Eng.*, 2022, **17**(5), 626–636.
3 J. Wang and R. Wang, Development of gas sensors and their applications in health safety, medical detection, and diagnosis, *Chemosensors*, 2025, **13**(5), 190.
4 J. Song, X. Lin, L. Y. Ee, S. F. Y. Li and M. Huang, A review on electrospinning as versatile supports for diverse nanofibers and their applications in environmental sensing, *Adv. Fiber Mater.*, 2023, **5**(2), 429–460.
5 A. Inobeme, A. Natarajan, S. Pradhan, C. O. Adetunji, A. I. Ajai, J. Inobeme, *et al.*, Chemical sensor technologies for sustainable development: recent advances, classification, and environmental monitoring, *Adv. Sens. Res.*, 2024, **3**(12), 2400066.
6 A. F. Danet, M.-C. Bratu, M.-C. Radulescu and A. Bratu, Portable minianalyzer based on cold vapor atomic absorption spectrometry at 184.9 nm for atmospheric mercury determination, *Sens. Actuators, B*, 2009, **137**(1), 12–16.
7 T. Qiang, C. Wang, M.-Q. Liu, K. K. Adhikari, J.-G. Liang, L. Wang, *et al.*, High-Performance porous MIM-type capacitive humidity sensor realized via inductive coupled

plasma and reactive-Ion etching, *Sens. Actuators, B*, 2018, **258**, 704–714.

8 X. Hao, W. Song, Y. Wang, J. Qin and Z. Jiang, Recent advancements in electrochemical sensors based on MOFs and their derivatives, *Small*, 2025, **21**(4), 2408624.

9 Y. Zhou, S. Xie, B. Liu, C. Wang, Y. Huang, X. Zhang, *et al.*, Chemiluminescence sensor for miRNA-21 detection based on CRISPR-Cas12a and cation exchange reaction, *Anal. Chem.*, 2023, **95**(6), 3332–3339.

10 J. Zhang, M. Zhou, X. Li, Y. Fan, J. Li, K. Lu, *et al.*, Recent advances of fluorescent sensors for bacteria detection-A review, *Talanta*, 2023, **254**, 124133. Available from: https://www.sciencedirect.com/science/article/pii/S0039914022009298.

11 N. Cao, J. Xu, H. Zhou, Y. Zhao, J. Xu, J. Li, *et al.*, A fluorescent sensor array based on silver nanoclusters for identifying heavy metal ions, *Microchem. J.*, 2020, **159**, 105406, DOI: 10.1016/j.microc.2020.105406.

12 Y. Shi, W. Li, X. Feng, L. Lin, P. Nie, J. Shi, *et al.*, Sensing of mercury ions in Porphyra by Copper @ Gold nanoclusters based ratiometric fluorescent aptasensor, *Food Chem.*, 2021, **344**, 128694.

13 M. Yang, C. Wang, Y. Yan, E. Liu, X. Hu, H. Hao, *et al.*, Visual detection of folic acid based on silica coated CdTeS quantum dots in serum samples, *Mater. Res. Bull.*, 2021, **144**, 111509, DOI: 10.1016/j.materresbull.2021.111509.

14 Z. Gan, T. Zhang, Y. Hu, S. Zhen and X. Hu, A simple fluorescence-scattering ratiometric sensor for biothiols based on CdTe quantum dots, *Sens. Actuators, B*, 2023, **378**, 133168.

15 Y. Cheng, H. Zhang, B. Yang, J. Wu, Y. Wang, B. Ding, *et al.*, Highly efficient fluorescence sensing of phosphate by dual-emissive lanthanide MOFs, *Dalton Trans.*, 2018, **47**(35), 12273–12283.

16 X. D. Zhu, K. Zhang, Y. Wang, W. W. Long, R. J. Sa and T. F. Liu, Fluorescent metal–organic framework (MOF) as a highly sensitive and quickly responsive chemical sensor for the detection of antibiotics in simulated wastewater, *Inorg. Chem.*, 2018, **57**(3), 1060–1065.

17 Y. Zhang, X. Yuan, X. Zhu, D. Zhang, H. Liu and B. Sun, Dandelion-like covalent organic frameworks with high-efficiency fluorescence for ratiometric sensing and visual tracking-by-detection of Fe3+, *Anal. Chim. Acta*, 2023, **1239**, 340671, DOI: 10.1016/j.aca.2022.340671.

18 K. F. Kayani, S. J. Mohammed, N. N. Mohammad, A. M. Abdullah, D. I. Tofiq, M. S. Mustafa, *et al.*, Sulfur quantum dots for fluorescence sensing in biological and pharmaceutical samples: a review, *Mater. Adv.*, 2024, **5**, 6351–6367, DOI: 10.1039/D4MA00502C.

19 N. Orachorn and O. Bunkoed, A nanocomposite fluorescent probe of polyaniline, graphene oxide and quantum dots incorporated into highly selective polymer for lomefloxacin detection, *Talanta*, 2019, **203**, 261–268.

20 R. Sedghi, H. Javadi, B. Heidari, A. Rostami and R. S. Varma, Efficient Optical and UV–Vis Chemosensor Based on Chromo Probes–Polymeric Nanocomposite Hybrid for Selective Recognition of Fluoride Ions, *ACS Omega*, 2019, **4**(14), 16001–16008.

21 X. Li, L. Pan, F. Yang and L. Yang, Blue Carbon Dot-Based Portable Smartphone Platform for Visualization of Copper(II), *ACS Appl. Nano Mater.*, 2022, **5**(7), 9252–9259.

22 C. Muñoz-Bustos, A. Tirado-Guízar, F. Paraguay-Delgado and G. Pina-Luis, Copper nanoclusters-coated BSA as a novel fluorescence sensor for sensitive and selective detection of mangiferin, *Sens. Actuators, B*, 2017, **244**, 922–927. Available from: https://www.sciencedirect.com/science/article/pii/S0925400517300783.

23 L. E. Kreno, K. Leong, O. K. Farha, M. Allendorf, R. P. Van Duyne and J. T. Hupp, Metal–organic framework materials as chemical sensors, *Chem. Rev.*, 2012, **112**(2), 1105–1125.

24 H. S. Al-mashriqi, P. Sanga, J. Chen, E. Qaed, J. Xiao, X. Li, *et al.*, Multifunctional Eu-doped carbon dots nanoprobe for highly sensitive and selective determination of glutathione in biological fluid and cell imaging, *Carbon*, 2024, **228**, 119380.

25 K. F. Kayani, S. J. Mohammed, N. N. Mohammad, G. H. Abdullah, D. A. Kader and N. S. Hamad Mustafa, Ratiometric fluorescence detection of tetracycline in milk and tap water with smartphone assistance for visual pH sensing using innovative dual-emissive phosphorus-doped carbon dots, *Food Control*, 2024, **164**, 110611.

26 M. K. Goshisht, G. K. Patra and N. Tripathi, Fluorescent Schiff base sensors as a versatile tool for metal ion detection: strategies, mechanistic insights, and applications, *Mater. Adv.*, 2022, **3**(6), 2612–2669.

27 K. F. Kayani, Portable smartphone-integrated ratiometric fluorescence probe for visual detection of mercury ions in environmental water with greenness evaluation, *RSC Adv.*, 2025, **15**(46), 38612–38623, DOI: 10.1039/D5RA06396E.

28 Z.-L. Chai, G.-H. Liu, Y.-R. Zheng, Y.-F. Ding, L. Wang, W.-K. Dong, *et al.*, A nonsymmetrical salamo-like fluorescence chemical sensor for selective identification of Cu2+ and B4O72− ions and practical applications, *Spectrochim. Acta, Part A*, 2024, **312**, 123839.

29 S. Ghosh, A. Rana and S. Biswas, Metal–organic framework-based fluorescent sensors for the detection of pharmaceutically active compounds, *Chem. Mater.*, 2023, **36**(1), 99–131.

30 X. Guo, L. Zhou, X. Liu, G. Tan, F. Yuan, A. Nezamzadeh-Ejhieh, *et al.*, Fluorescence detection platform of metal-organic frameworks for biomarkers, *Colloids Surf., B*, 2023, **229**, 113455.

31 A. MP, S. Pardhiya and P. Rajamani, Carbon dots: an excellent fluorescent probe for contaminant sensing and remediation, *Small*, 2022, **18**(15), 2105579.

32 K. F. Kayani, Carbon Dots: Synthesis, Characterization, and Applications in the Detection of Bilirubin – Recent Advances and Challenges, *J. Fluoresc.*, 2025, **35**, 11231–11247.

33 K. A. Othman, L. I. A. Ali, A. F. Qader, R. A. Omer and A. A. Amin, Synthesis, characterization, and applications of carbon dots for determination of pharmacological and

biological samples: a review, *J. Fluoresc.*, 2025, **35**(5), 2511–2525.

34 S. Ross, R. S. Wu, S. C. Wei, G. M. Ross and H. T. Chang, The analytical and biomedical applications of carbon dots and their future theranostic potential: A review, *J. Food Drug Anal.*, 2020, **28**(4), 677–695.

35 C. He, P. Xu, X. Zhang and W. Long, The synthetic strategies, photoluminescence mechanisms and promising applications of carbon dots: Current state and future perspective, *Carbon*, 2022, **186**, 91–127.

36 M. K. Barman, B. Jana, S. Bhattacharyya and A. Patra, Photophysical properties of doped carbon dots (N, P, and B) and their influence on electron/hole transfer in carbon dots–nickel (II) phthalocyanine conjugates, *J. Phys. Chem. C*, 2014, **118**(34), 20034–20041.

37 G. Jeong, C. H. Park, D. Yi and H. Yang, Green synthesis of carbon dots from spent coffee grounds via ball-milling: Application in fluorescent chemosensors, *J. Cleaner Prod.*, 2023, **392**, 136250. Available from: https://www.sciencedirect.com/science/article/pii/S0959652623004080.

38 J. Joseph and A. A. Anappara, White-light-emitting carbon dots prepared by the electrochemical exfoliation of graphite, *ChemPhysChem*, 2017, **18**(3), 292–298.

39 C. He, H. Yan, X. Li and X. Wang, In situ fabrication of carbon dots-based lubricants using a facile ultrasonic approach, *Green Chem.*, 2019, **21**(9), 2279–2285.

40 J. Park, P. Bazylewski, V. Wong, H. Shah and G. Fanchini, Solvent-free growth of carbon dots by sputter-plasma assisted chemical vapour deposition over large areas, *Carbon*, 2019, **146**, 28–35.

41 Y. Zhao, S. Jing, X. Peng, Z. Chen, Y. Hu, H. Zhuo, *et al.*, Synthesizing green carbon dots with exceptionally high yield from biomass hydrothermal carbon, *Cellulose*, 2020, **27**(1), 415–428.

42 V. Bressi, A. M. Balu, D. Iannazzo and C. Espro, Recent advances in the synthesis of carbon dots from renewable biomass by high-efficient hydrothermal and microwave green approaches, *Curr. Opin. Green Sustainable Chem.*, 2023, **40**, 100742.

43 K. F. Kayani, S. J. Mohammed, D. Ghafoor, M. K. Rahim and H. R. Ahmed, Carbon dot as fluorescence sensor for glutathione in human serum samples: a review, *Mater. Adv.*, 2024, **5**(11), 4618–4633, DOI: 10.1039/D4MA00185K.

44 R. Aslam, Q. Wang, R. Wang and Z. Yan, Synthesis Methodology of Carbon Dots: Modern Trends and Enhancements, *Nano-Hybrid Smart Coatings: Advancements in Industrial Efficiency and Corrosion Resistance*, 2024, pp. 95–120.

45 K. F. Kayani, Metal-doped carbon dots for sensing applications in food analysis: A critical review, *Microchem. J.*, 2025, **215**, 114296. Available from: https://www.sciencedirect.com/science/article/pii/S0026265X25016509.

46 S. J. Mohammed, M. K. Sidiq, H. H. Najmuldeen, K. F. Kayani, D. A. Kader and S. B. Aziz, A Comprehensive Review on Nitrogen-Doped Carbon Dots for Antibacterial Applications, *J. Environ. Chem. Eng.*, 2024, **12**(6), 114444. Available from: https://www.sciencedirect.com/science/article/pii/S2213343724025752.

47 F. Akhter, J. Ahmed, M. A. Pinjaro, F. A. Shaikh, H. J. Arain and M. J. Ahsan, Metal-doped carbon dots (MCDs) as efficient nano-adsorbents for detection, monitoring, and degradation of wastewater pollutants: recent progress, challenges, and future prospects, *Water, Air, Soil Pollut.*, 2023, **234**(11), 672.

48 W. Chen, A. S. Ball, I. Cole and H. Yin, Metal-Doped Carbon Dots as Fenton-like Catalysts and Their Applications in Pollutant Degradation and Sensing, *Sustainability*, 2025, **17**(8), 3642.

49 K. Jian, W. Men, C. Miao, Y. Du, H. Yang and X. Zhao, Fe-doped carbon dots with enhanced fluorescence: Facilitating Cu2+ detection and urea electro-oxidation, *Talanta*, 2025, **292**, 127942. Available from: https://www.sciencedirect.com/science/article/pii/S0039914025004321.

50 L. Zhang, Y. Hao, Y. Liu, Y. Dong, Z. Chen, W. Dong, *et al.*, Nickel doping: Improving the optical properties of carbon dots and increasing the sensitivity for detecting pH and water, *J. Alloys Compd.*, 2024, **976**, 173131. Available from: https://www.sciencedirect.com/science/article/pii/S0925838823044341.

51 X. Chu, G. Ning, Z. Zhou, Y. Liu, Q. Xiao and S. Huang, Bright Mn-doped carbon dots for the determination of permanganate and L-ascorbic acid by a fluorescence on-off-on strategy, *Microchim. Acta*, 2020, **187**(12), 659.

52 X. Wang, Z. Cheng, Y. Zhou, S. K. Tammina and Y. Yang, A double carbon dot system composed of N, Cl-doped carbon dots and N, Cu-doped carbon dots as peroxidase mimics and as fluorescent probes for the determination of hydroquinone by fluorescence, *Microchim. Acta*, 2020, **187**(6), 350.

53 S. E. Bodman and S. J. Butler, Advances in anion binding and sensing using luminescent lanthanide complexes, *Chem. Sci.*, 2021, **12**(8), 2716–2734.

54 X. Liu, H. Wang, D. Yang, F. Jing, H. Qiu, H. Liu, *et al.*, Embedded lanthanoid ions modulated the periodic luminescence of transition metal dichalcogenide monolayers prepared from an aqueous orecursor, *J. Mater. Chem. C*, 2022, **10**(20), 8061–8069.

55 X. Li, J. Gao, S. Rao and Y. Zheng, Development of a selective "on-off-on" nano-sensor based on lanthanide encapsulated carbon dots, *Synth. Met.*, 2017, **231**, 107–111. Available from: https://www.sciencedirect.com/science/article/pii/S0379677917301959.

56 Z. Xu, J. Chen, Y. Liu, X. Wang and Q. Shi, Multi-emission fluorescent sensor array based on carbon dots and lanthanide for detection of heavy metal ions under stepwise prediction strategy, *Chem. Eng. J.*, 2022, **441**, 135690. Available from: https://www.sciencedirect.com/science/article/pii/S1385894722011901.

57 H. X. Zhao, L. Q. Liu, Z. De Liu, Y. Wang, X. J. Zhao and C. Z. Huang, Highly selective detection of phosphate in very complicated matrixes with an off–on fluorescent

probe of europium-adjusted carbon dots, *Chem. Commun.*, 2011, **47**(9), 2604–2606.
58 F. Li, D. Yang and H. Xu, Non-metal-heteroatom-doped carbon dots: synthesis and properties, *Chem.–Eur. J.*, 2019, **25**(5), 1165–1176.
59 S. Miao, K. Liang, J. Zhu, B. Yang, D. Zhao and B. Kong, Hetero-atom-doped carbon dots: Doping strategies, properties and applications, *Nano Today*, 2020, **33**, 100879.
60 X. Li, Y. Fu, S. Zhao, J. Xiao, M. Lan, B. Wang, *et al.*, Metal ions-doped carbon dots: Synthesis, properties, and applications, *Chem. Eng. J.*, 2022, **430**, 133101.
61 S. Munusamy, T. R. Mandlimath, P. Swetha, A. G. Al-Sehemi, M. Pannipara, S. Koppala, *et al.*, Nitrogen-doped carbon dots: Recent developments in its fluorescent sensor applications, *Environ. Res.*, 2023, **231**, 116046.
62 Q. Fu, S. Sun, K. Lu, N. Li and Z. Dong, Boron-doped carbon dots: Doping strategies, performance effects, and applications, *Chin. Chem. Lett.*, 2024, **35**(7), 109136.
63 K. F. Kayani, Phosphorus-doped carbon dots and their analytical and bioanalytical applications: a review, *Talanta*, 2026, **297**, 128768.
64 L. G. Nielsen, A. K. R. Junker and T. J. Sørensen, Composed in the f-block: solution structure and function of kinetically inert lanthanide (III) complexes, *Dalton Trans.*, 2018, **47**(31), 10360–10376.
65 Y. Hasegawa, Y. Wada and S. Yanagida, Strategies for the design of luminescent lanthanide(III) complexes and their photonic applications, *J. Photochem. Photobiol., C*, 2004, **5**(3), 183–202.
66 A. Chandrasekar, M. Joshi and T. K. Ghanty, On the position of La, Lu, Ac and Lr in the periodic table: a perspective, *J. Chem. Sci.*, 2019, **131**(12), 122.
67 D. Mouchel Dit Leguerrier, R. Barré, J. K. Molloy and F. Thomas, Lanthanide complexes as redox and ROS/RNS probes: A new paradigm that makes use of redox-reactive and redox non-innocent ligands, *Coord. Chem. Rev.*, 2021, **446**, 214133.
68 T. Madanhire, L.-C. C. Coetzee, T. J. Rashamuse and N. P. Magwa, Beyond the norm: Exploring the unusual oxidation states of lanthanides (+1, +II, +IV and +V) and their potential applications, *Inorg. Chem. Commun.*, 2025, **176**, 114218.
69 S. SeethaLekshmi, A. R. Ramya, M. L. P. Reddy and S. Varughese, Lanthanide complex-derived white-light emitting solids: A survey on design strategies, *J. Photochem. Photobiol., C*, 2017, **33**, 109–131.
70 E. G. Moore, A. P. S. Samuel and K. N. Raymond, From Antenna to Assay: Lessons Learned in Lanthanide Luminescence, *Acc. Chem. Res.*, 2009, **42**(4), 542–552, DOI: 10.1021/ar800211j.
71 X. Wang, H. Chang, J. Xie, B. Zhao, B. Liu, S. Xu, *et al.*, Recent developments in lanthanide-based luminescent probes, *Coord. Chem. Rev.*, 2014, **273–274**, 201–212.
72 J. Rocha, L. D. Carlos, F. A. A. Paz and D. Ananias, Luminescent multifunctional lanthanides-based metal–organic frameworks, *Chem. Soc. Rev.*, 2011, **40**(2), 926–940.
73 S. Afzal and U. Maitra, Sensitized Lanthanide Photoluminescence Based Sensors–a Review, *Helv. Chim. Acta*, 2022, **105**(2), e202100194.
74 I. F. Costa, L. Blois, T. B. Paolini, I. P. Assunção, E. E. S. Teotonio, M. C. F. C. Felinto, *et al.*, Luminescence properties of lanthanide tetrakis complexes as molecular light emitters, *Coord. Chem. Rev.*, 2024, **502**, 215590.
75 Q. Xu, T. Kuang, Y. Liu, L. Cai, X. Peng, T. Sreenivasan Sreeprasad, *et al.*, Heteroatom-doped carbon dots: synthesis, characterization, properties, photoluminescence mechanism and biological applications, *J. Mater. Chem. B*, 2016, **4**, 7204–7219.
76 Z. Zhang, G. Yi, P. Li, X. Zhang, H. Fan, Y. Zhang, *et al.*, A minireview on doped carbon dots for photocatalytic and electrocatalytic applications, *Nanoscale*, 2020, **12**(26), 13899–13906, DOI: 10.1039/D0NR03163A.
77 F. Yan, Y. Jiang, X. Sun, Z. Bai, Y. Zhang and X. Zhou, Surface modification and chemical functionalization of carbon dots: a review, *Microchim. Acta*, 2018, **185**, 1–34.
78 H. Wang, L. Ai, Z. Song, M. Nie, J. Xiao, G. Li, *et al.*, Surface modification functionalized carbon dots, *Chem.–Eur. J.*, 2023, **29**(65), e202302383.
79 L. Liang, S. Cai, Y. Leng, C. Huang, Y. Liu, Y. Wang, *et al.*, Intelligent sensing platform based on europium-doped carbon dots for dual-functional detection of ciprofloxacin/Ga3+ and its tracking in vivo, *J. Hazard. Mater.*, 2025, **483**, 136622.
80 R. Yao, Z. Li, P. Huo, C. Gong, J. Li, C. Fan, *et al.*, A Eu3+-based high sensitivity ratiometric fluorescence sensor for determination of tetracycline combining bi-functional carbon dots by surface functionalization and heteroatom doping, *Dyes Pigm.*, 2022, **201**, 110190.
81 Q. Fu, S. Sun, N. Li, K. Lu and Z. Dong, Based on halogen-doped carbon dots: A review, *Mater. Today Chem.*, 2023, **34**, 101769.
82 R. Yu, M. Ou, Q. Hou, C. Li, S. Qu and Z. Tan, Metal and non-metal doped carbon dots: properties and applications, *Light Adv. Manuf.*, 2025, **5**(4), 647–666.
83 A. Kumar, P. Singh, P. Kumari, K. Nidhi, R. K. Singh, S. K. Sahu, *et al.*, Design of lanthanide-doped carbon dots Nanochemosensor for Paper-strip based as well as in-vitro Turn-off–on detection of Fe2+ ions and hydrogen peroxide, *Spectrochim. Acta, Part A*, 2025, 126282.
84 Y. Deng, M. Chen, G. Chen, W. Zou, Y. Zhao, H. Zhang, *et al.*, Visible-Ultraviolet Upconversion Carbon Quantum Dots for Enhancement of the Photocatalytic Activity of Titanium Dioxide, *ACS Omega*, 2021, **6**(6), 4247–4254.
85 C. Liu, Y. Mei, Q. Lei, X. Ma, X. Nan, Y. Zhu, *et al.*, Fluorescent carbon dots based on food wastes: Applications in food safety detection, *Chem. Eng. J.*, 2024, **499**, 156434.
86 J. Zhang, B. Zhang, A. Xia, Q. Zhou, X. Zhu, Y. Huang, *et al.*, Production of carbon dots, biofuels, bio-adsorbents, and biological nutrients via hydrothermal conversion of Chlorella pyrenoidosa and oilseed rape straw, *Biochar*, 2025, **7**(1), 109, DOI: 10.1007/s42773-025-00482-y.

87 Y. Wang, Y. Zhu, S. Yu and C. Jiang, Fluorescent carbon dots: Rational synthesis, tunable optical properties and analytical applications, *RSC Adv.*, 2017, **7**(65), 40973–40989.
88 P. Zuo, X. Lu, Z. Sun, Y. Guo and H. He, A review on syntheses, properties, characterization and bioanalytical applications of fluorescent carbon dots, *Microchim. Acta*, 2016, **183**(2), 519–542.
89 X. Tian and X. Yin, Carbon dots, unconventional preparation strategies, and applications beyond photoluminescence, *Small*, 2019, **15**(48), 1901803.
90 J. Bian, Z. Wang, J. Ge, W. Gong, K. Nan, Z. Liu, *et al.*, Recent advances of fluorescent carbon dots for biological imaging and biosensing, *Chem. Eng. J.*, 2025, **519**, 165135.
91 Q. Zhao, W. Song, B. Zhao and B. Yang, Spectroscopic studies of the optical properties of carbon dots: recent advances and future prospects, *Mater. Chem. Front.*, 2020, **4**(2), 472–488, DOI: 10.1039/C9QM00592G.
92 N. Javed and D. M. O'Carroll, Carbon Dots and Stability of Their Optical Properties, *Part. Part. Syst. Charact.*, 2021, **38**(4), 1–12.
93 K. F. Kayani, M. K. Rahim, S. J. Mohammed, H. R. Ahmed, M. S. Mustafa and S. B. Aziz, Recent Progress in Folic Acid Detection Based on Fluorescent Carbon Dots as Sensors: A Review, *J. Fluoresc.*, 2024, **35**, 2481–2494.
94 L. Shi, J. H. Yang, H. B. Zeng, Y. M. Chen, S. C. Yang, C. Wu, *et al.*, Carbon dots with high fluorescence quantum yield: The fluorescence originates from organic fluorophores, *Nanoscale*, 2016, **8**(30), 14374–14378.
95 X. Tian and Z. Fan, Comparison between terbium-doped carbon dots and terbium-functionalized carbon dots: Characterization, optical properties, and applications in anthrax biomarker detection, *J. Lumin.*, 2022, **244**, 118732.
96 F. Wu, H. Su, X. Zhu, K. Wang, Z. Zhang and W.-K. Wong, Near-infrared emissive lanthanide hybridized carbon quantum dots for bioimaging applications, *J. Mater. Chem. B*, 2016, **4**(38), 6366–6372.
97 J. Dai and X. Zhang, Chemical regulation of fluorescence lifetime, *Chem. Biomed. Imaging*, 2023, **1**(9), 796–816.
98 C. Zheng, X. An and J. Gong, Novel pH sensitive N-doped carbon dots with both long fluorescence lifetime and high quantum yield, *RSC Adv.*, 2015, **5**(41), 32319–32322.
99 M. S. Mustafa and W. O. Karim, Environmentally friendly fluorescence platform for detection of tetracycline in pharmaceutical formulations and human serums based on highly fluorescent 1,4-di-2-(5-phenyloxazolyl)-benzene, *RSC Adv.*, 2026, **16**(15), 13320–13331, DOI: 10.1039/D6RA00893C.
100 H. Wu, Y. Chen, M. Xu, Y. Ling, S. Ju, Y. Tang, *et al.*, Dual-response fluorescent probe based on nitrogen-doped carbon dots and europium ions hybrid for ratiometric and on-site visual determination of oxytetracycline and tetracycline, *Sci. Total Environ.*, 2023, **860**, 160533.
101 Y. Meng, X. Sun, J. Xing and C. Dong, Eu3+ doped carbon dots as a ratiometric fluorescence probe for highly sensitive detection of trace tetracycline in milk, *Spectrochim. Acta, Part A*, 2026, **345**, 126811.
102 Y. Yan, H. Guo, Z. Yu, Z. Yang, R. Yan, Y. Ma, *et al.*, Encapsulating boron-doped carbon dots into Eu-MOF as a ratiometric fluorescence probe for the rapid detection of caffeic acid, *J. Environ. Chem. Eng.*, 2025, **13**(3), 117129.
103 X. Sun and Y. Lei, Fluorescent carbon dots and their sensing applications, *TrAC, Trends Anal. Chem.*, 2017, **89**, 163–180, DOI: 10.1016/j.trac.2017.02.001.
104 K. F. Kayani, D. Ghafoor, S. J. Mohammed and O. B. A. Shatery, Carbon dots: synthesis, sensing mechanisms, and potential applications as promising materials for glucose sensors, *Nanoscale Adv.*, 2025, **7**(1), 42–59, DOI: 10.1039/D4NA00763H.
105 J. Tian, M. An, X. Zhao, Y. Wang and M. Hasan, Advances in fluorescent sensing carbon dots: An account of food analysis, *ACS Omega*, 2023, **8**(10), 9031–9039.
106 H. Zhang, Q. Zhang, N. Li, G. Yang, Z. Cheng, X. Du, *et al.*, Advances in the application of carbon dots-based fluorescent probes in disease biomarker detection, *Colloids Surf., B*, 2025, **245**, 114360.
107 K. F. Kayani and S. J. Mohammed, Heavy metal pollution in aquatic environments and removal using highly efficient bimetallic metal–organic framework adsorbents, *RSC Adv.*, 2025, **15**(43), 35756–35769, DOI: 10.1039/D5RA06296A.
108 E. B. Hussein, F. A. Rasheed, A. S. Mohammed and K. F. Kayani, Emerging nanotechnology approaches for sustainable water treatment and heavy metals removal: a comprehensive review, *RSC Adv.*, 2025, **15**(48), 41061–41107, DOI: 10.1039/D5RA06914A.
109 X.-Y. Xu and B. Yan, Fabrication and application of a ratiometric and colorimetric fluorescent probe for Hg 2+ based on dual-emissive metal–organic framework hybrids with carbon dots and Eu 3+, *J. Mater. Chem. C*, 2016, **4**(7), 1543–1549.
110 Y. Sang, K. Wang, X. Kong, F. Cheng, C. Zhou and W. Li, Color-multiplexing europium doped carbon dots for highly selective and dosage-sensitive cascade visualization of tetracycline and Al3+, *Sens. Actuators, B*, 2022, **362**, 131780.
111 M. L. Desai, S. Jha, H. Basu, R. K. Singhal, P. K. Sharma and S. K. Kailasa, Microwave-assisted synthesis of water-soluble Eu 3+ hybrid carbon dots with enhanced fluorescence for the sensing of Hg 2+ ions and imaging of fungal cells, *New J. Chem.*, 2018, **42**(8), 6125–6133.
112 C. Correia, J. Martinho and E. Maçôas, A fluorescent nanosensor for silver (Ag+) and mercury (Hg2+) ions using Eu (III)-doped carbon dots, *Nanomaterials*, 2022, **12**(3), 385.
113 Z. Zhang, J. Li, X. Wang, A. Liang and Z. Jiang, Aptamer-mediated N/Ce-doped carbon dots as a fluorescent and resonance Rayleigh scattering dual mode probe for arsenic (III), *Microchim. Acta*, 2019, **186**(9), 638.
114 S. Mohandoss, A. Priyadharshini, K. S. Velu, A. A. Napoleon, P. Roy, N. Ahmad, *et al.*, A reversible photoluminescence based on cerium-doped carbon dots for "on–off-on" dual detection of Fe3+ and pyrophosphate ions with live cell application, *Inorg. Chem. Commun.*, 2025, 114824.

115 S. Q. Chai, J. H. He, L. Zhan, Y. F. Li, C. M. Li and C. Z. Huang, Dy (III)-induced aggregation emission quenching effect of single-layered graphene quantum dots for selective detection of phosphate in the artificial wetlands, *Talanta*, 2019, **196**, 100–108.

116 S. Mohandoss, R. Tamizhselvi, K. S. Velu, A. A. Napoleon, M. Aslam, N. Ahmad, *et al.*, Facile hydrothermal synthesis of Gd-doped carbon quantum dots for dual-mode colorimetric and photoluminescence sensing of Hg2+ ions with potential real samples and bioimaging applications, *Inorg. Chem. Commun.*, 2025, 114689.

117 D. Zhao, C. Zhang, H. Liu, Y. Jiao and X. Xiao, Gadolinium-doped carbon dots with dual enzyme activity for visual detection of Cu2+ and antibacterial applications, *ACS Appl. Nano Mater.*, 2024, **7**(4), 4228–4238.

118 M. Zhang, W. Wang, P. Yuan, C. Chi, J. Zhang and N. Zhou, Synthesis of lanthanum doped carbon dots for detection of mercury ion, multi-color imaging of cells and tissue, and bacteriostasis, *Chem. Eng. J.*, 2017, **330**, 1137–1147, DOI: 10.1016/j.cej.2017.07.166.

119 X. Zhang, J. Wu, M. Wu, L. Wang, D. Yu, N. Yan, *et al.*, Non-cytotoxic lanthanum and nitrogen co-doped lignin-based carbon dots for selective detection of ions in biological imaging, *J. Environ. Chem. Eng.*, 2023, **11**(3), 109881.

120 S. Yang, X. Sun, Z. Wang, X. Wang, G. Guo and Q. Pu, Anomalous enhancement of fluorescence of carbon dots through lanthanum doping and potential application in intracellular imaging of ferric ion, *Nano Res.*, 2018, **11**(3), 1369–1378.

121 T. K. Mondal, S. Mondal, U. K. Ghorai and S. K. Saha, White light emitting lanthanide based carbon quantum dots as toxic Cr (VI) and pH sensor, *J. Colloid Interface Sci.*, 2019, **553**, 177–185.

122 S. Mohandoss, P. Roy, N. Ahmad, K. S. Velu, S. Palanisamy, M. Aslam, *et al.*, Facile synthesis of dual rare earth metal-doped carbon quantum dots as photoluminescent sensors for ag+ and Hg2+ detection with intracellular bioimaging applications, *J. Photochem. Photobiol., A*, 2025, 116823.

123 B. Li, F. Wu, Z. Xie, X. Kang, Y. Wang, W. Li, *et al.*, High acid-base tolerance and long storage time lanthanum cerium co-doped carbon quantum dots for Fe3+ detection, *Spectrochim. Acta, Part A*, 2025, **327**, 125403.

124 S. Mohandoss, A. Priyadharshini, K. S. Velu, A. A. Napoleon, P. Roy, N. Ahmad, *et al.*, Rare-earth metal-doped orange emissive photoluminescent carbon quantum dots for highly sensitive detection of Hg2+ ions: Multi-color imaging and real samples, *Mater. Sci. Eng., B*, 2025, **317**, 118236.

125 X. He, Y. Han, X. Luo, W. Yang, C. Li, W. Tang, *et al.*, Terbium (III)-referenced N-doped carbon dots for ratiometric fluorescent sensing of mercury (II) in seafood, *Food Chem.*, 2020, **320**, 126624.

126 K. F. Kayani, Molecularly imprinted polymer-combined with metal organic frameworks (MIP/MOFs) for ratiometric fluorescence sensing applications, *Talanta*, 2026, **299**, 129142.

127 Z. Li, Y. Wang, J. Chen, L. Zhang, Y. Hua, D. Huang, *et al.*, Ratiometric fluorescent probes based on carbon dots and europium for rapid detection of tetracycline, *Opt. Mater.*, 2024, **150**, 115227.

128 M. Liu, S. Wei, Y. Xie, K. Su, X. Yin, X. Song, *et al.*, Ratiometric fluorescence sensor based on chiral europium-doped carbon dots for specific and portable detection of tetracycline, *Sens. Actuators, B*, 2025, **423**, 136753.

129 L. Ma, F. Wang, Y. Hua, Q. Chen, M. Zhang, Q. Zhao, *et al.*, A ratiometric fluorescent nanoprobe for the specific and portable detection of tetracycline based on Eu/N, S-doped carbon dots, *Spectrochim. Acta, Part A*, 2025, 127063.

130 H. Hu, H. Xing, Y. Zhang, X. Liu, S. Gao, L. Wang, *et al.*, Centrifugated lateral flow assay strips based on dual-emission carbon dots modified with europium ions for ratiometric determination and on-site discrimination of tetracyclines in environment, *Sci. Total Environ.*, 2024, **951**, 175478.

131 A. Babenova, K. Zhumanova, A. Zhussupbekova, K. Zhussupbekov, D. Tosi and T. S. Atabaev, Excitation Wavelength Optimization of Europium-Doped Carbon Dots (Eu-CDs) for Highly Sensitive Detection of Tetracyclines in Water, *ACS Omega*, 2024, **10**(1), 619–626.

132 Y. J. Fan, Z. G. Wang, M. Su, X. T. Liu, S. G. Shen and J. X. Dong, A dual-signal fluorescent colorimetric tetracyclines sensor based on multicolor carbon dots as probes and smartphone-assisted visual assay, *Anal. Chim. Acta*, 2023, **1247**, 340843.

133 T.-T. Zhang, Z.-H. Chen, G.-Y. Shi and M. Zhang, Eu3+-doped bovine serum albumin-derived carbon dots for ratiometric fluorescent detection of tetracycline, *J. Anal. Test.*, 2022, **6**(4), 365–373.

134 Y. Meng, X. Sun, J. Xing and C. Dong, Eu3+ doped carbon dots as a ratiometric fluorescence probe for highly sensitive detection of trace tetracycline in milk, *Spectrochim. Acta, Part A*, 2025, 126811.

135 X. Sun, M. Jiang, L. Chen and N. Niu, Construction of ratiometric fluorescence MIPs probe for selective detection of tetracycline based on passion fruit peel carbon dots and europium, *Microchim. Acta*, 2021, **188**(9), 297.

136 X. Cui, T. Lei, J. Zhang, Z. Chen, H. Luo, H. Chen, *et al.*, Smartphone-assisted miniature device based on nitrogen and sulfur co-doped carbon dots for point-of-care testing of tetracycline, *Spectrochim. Acta, Part A*, 2022, **283**, 121727.

137 L. Jia, R. Chen, J. Xu, L. Zhang, X. Chen, N. Bi, *et al.*, A stick-like intelligent multicolor nano-sensor for the detection of tetracycline: The integration of nano-clay and carbon dots, *J. Hazard. Mater.*, 2021, **413**, 125296, DOI: 10.1016/j.jhazmat.2021.125296.

138 K. Arkin, Y. Zheng, Y. Bei, X. Ma, W. Che and Q. Shang, Construction of dual-channel ratio sensing platform and molecular logic gate for visual detection of oxytetracycline based on biomass carbon dots prepared from cherry tomatoes stalk, *Chem. Eng. J.*, 2023, **464**, 142552.

139 W. Hou, C. Liang, Y. Li, C. Shao, Y. Zheng, Z. Li, *et al.*, A fluorescence sensor based on surface functionalization and heteroatom co-doped carbon dots for detection of tetracycline, *J. Photochem. Photobiol., A*, 2025, **466**, 116411.

140 W. Li, J. Zhu, G. Xie, Y. Ren and Y.-Q. Zheng, Ratiometric system based on graphene quantum dots and Eu3+ for selective detection of tetracyclines, *Anal. Chim. Acta*, 2018, **1022**, 131–137.

141 Z. Shen, C. Zhang, X. Yu, J. Li, Z. Wang, Z. Zhang, *et al.*, Microwave-assisted synthesis of cyclen functional carbon dots to construct a ratiometric fluorescent probe for tetracycline detection, *J. Mater. Chem. C*, 2018, **6**(36), 9636–9641, DOI: 10.1039/C8TC02982B.

142 H. Wu, M. Xu, Y. Chen, H. Zhang, Y. Shen and Y. Tang, A highly sensitive and selective nano-fluorescent probe for ratiometric and visual detection of oxytetracycline benefiting from dual roles of nitrogen-doped carbon dots, *Nanomaterials*, 2022, **12**(23), 4306.

143 Z. Wang, H. Xu, L. Wang, X. Zheng, T. Zhao, B. Qu, *et al.*, Highly-sensitive ratiometric determination of tetracyclines and smartphone-assisted visual assay by carrot-derived nitrogen-doped carbon dots-europium ion dual-emission fluorescence probe, *Microchem. J.*, 2025, **212**, 113398.

144 X. Lu, Q. Gao, L. Xu, Y. Ren, F. Tong, Y. Wang, *et al.*, Rapid determination of tetracycline utilizing a ratiometric fluorescence with Co-doped carbon quantum dots, *J. Food Compos. Anal.*, 2025, **140**, 107252.

145 J. Zhang, Y. Chen, J. Qi, Q. Miao, D. Deng, H. He, *et al.*, A paper-based ratiometric fluorescence sensor based on carbon dots modified with Eu 3+ for the selective detection of tetracycline in seafood aquaculture water, *Analyst*, 2024, **149**(5), 1571–1578.

146 Q. Wang, X. Li, K. Yang, S. Zhao, S. Zhu, B. Wang, *et al.*, Carbon dots and Eu3+ hybrid-based ratiometric fluorescent probe for oxytetracycline detection, *Ind. Eng. Chem. Res.*, 2022, **61**(17), 5825–5832.

147 Y. Li, K. Feng, M. Li, H. Li, W. Zhang, X. Yang, *et al.*, A dual-mode ratiometric probe using europium-doped cyclen-functional carbon dots for fluorescent and point-of-care detection of tetracycline, *Environ. Technol.*, 2024, **45**(28), 6051–6059.

148 Y. J. Fan, M. Su, Y.-E. Shi, X. T. Liu, S. G. Shen and J. X. Dong, A ratiometric fluorescent sensor for tetracyclines detection in meat based on pH-dependence of targets with lanthanum-doped carbon dots as probes, *Anal. Bioanal. Chem.*, 2022, **414**(8), 2597–2606.

149 P.-X. Yuan, J. Qin, J.-W. Zhang, J. Bai, S. Yang, D. Liao, *et al.*, Deep learning-assisted accurate sensing and discrimination of fluoroquinolone antibiotics based on terbium-doped carbon dots, *Microchem. J.*, 2025, 114674.

150 R. Ali, R. Alshaman, A. S. Albalawi, O. M. Alsharif, O. A. Hakami, H. H. Alharthi, *et al.*, Fluorometric detection of quinolones via AIE and FRET with terbium-doped carbon dots and copper nanoclusters, *Food Chem.*, 2025, **465**, 142076.

151 A. Serag, F. M. Almutairi, M. M. Aldhafeeri, R. M. Alzhrani, M. H. Abduljabbar, R. M. Alnemari, *et al.*, Ultrasensitive detection of alogliptin via fluorescence quenching of terbium-doped carbon quantum dots: mechanistic investigation, Box–Behnken optimization and analytical evaluation, *RSC Adv.*, 2025, **15**(24), 19468–19479.

152 Y. F. Hassan, E. Alzahrani, R. E. Saraya, M. A. Abdel-Lateef, E. A. M. El-Shoura, H. A. Batakoushy, *et al.*, A promising green fluorimetric approach for analysis of edoxaban in real human plasma using green carbon dots decorated with terbium ions, *Chem. Pap.*, 2025, **79**(1), 497–510.

153 F. Latifi, M. Amjadi, T. Hallaj and S. M. S. Alavi, Tb doped carbon dots as a platform for fluorescence ratiometric and colorimetric sensor for deferasirox, *Sci. Rep.*, 2025, **15**(1), 18075.

154 M. A. Abdel-Lateef, M. A. Albalawi, S. N. Al-Ghamdi, W. A. Mahdi, S. Alshehri and M. A. El Hamd, Determination of metanil yellow dye in turmeric powder using a unique fluorescence Europium doped carbon dots, *Spectrochim. Acta, Part A*, 2023, **287**, 122124.

155 C. Zhang, H. Zhang, Y. Yu, S. Wu and F. Chen, Ratio fluorometric determination of ATP base on the reversion of fluorescence of calcein quenched by Eu (III) ion using carbon dots as reference, *Talanta*, 2019, **197**, 451–456.

156 H. Zhang, Q. Zhang, J. Tang, H. Yang, X. Ji, J. Wang, *et al.*, A Portable and Thermally Degradable Hydrogel Sensor Based on Eu-Doped Carbon Dots for Visual and Ultrasensitive Detection of Ferric Ion, *Molecules*, 2025, **30**(15), 3280.

157 S.-J. Qin and B. Yan, Dual-emissive ratiometric fluorescent probe based on Eu3+/C-dots@ MOF hybrids for the biomarker diaminotoluene sensing, *Sens. Actuators, B*, 2018, **272**, 510–517.

158 N. Amin, A. Afkhami and T. Madrakian, Construction of a novel "Off-On" fluorescence sensor for highly selective sensing of selenite based on europium ions induced crosslinking of nitrogen-doped carbon dots, *J. Lumin.*, 2018, **194**, 768–777.

159 X. Zhou, Y. Wang, J. Song, L. Xiong, X. Zhao, S. Chen, *et al.*, Engineering fluorescent carbon dot sensor with rare earth europium for the detection of uranium (VI) ion in vivo, *Microchim. Acta*, 2025, **192**(4), 1–12.

160 M. A. Albalawi, H. Gomaa, M. A. El Hamd, M. A. S. Abourehab and M. A. Abdel-Lateef, Detection of indigo carmine dye in juices via application of photoluminescent europium-doped carbon dots from tannic acid, *Luminescence*, 2023, **38**(2), 92–98.

161 X. Tian and Z. Fan, A design strategy of ratiometric probe based on dual-colored carbon dots for phosphate detection, *Dyes Pigm.*, 2024, **223**, 111935.

162 B. B. Chen, Z. X. Liu, H. Y. Zou and C. Z. Huang, Highly selective detection of 2, 4, 6-trinitrophenol by using newly developed terbium-doped blue carbon dots, *Analyst*, 2016, **141**(9), 2676–2681.

163 Y. A. B. Jardan, A. M. Mostafa, J. Barker, M. N. Goda, A. B. H. Ali and M. M. El-Wekil, Engineering sensitive ratiometric probe based on Tb@ BNCDs and thiolated-protected AuNCs for melamine sensing via competitive coordination mechanism, *Microchim. Acta*, 2025, **192**(8), 531.

164 A. K. Goel, Anthrax: A disease of biowarfare and public health importance, *World J. Clin. Cases*, 2015, **3**(1), 20.
165 P.-P. Zhang, A.-Y. Ni, J.-J. Zhang, B.-L. Zhang, H. A. Zhou, H. Zhao, *et al.*, Tb-MOF-based luminescent recovery probe for rapid and facile detection of an anthrax biomarker, *Sens. Actuators, B*, 2023, **384**, 133624.
166 K. F. Kayani, O. B. A. Shatery, S. J. Mohammed, H. R. Ahmed, R. F. Hamarawf and M. S. Mustafa, Synthesis and applications of luminescent metal organic frameworks (MOFs) for sensing dipicolinic acid in biological and water samples: a review, *Nanoscale Adv.*, 2025, **7**(1), 13–41, DOI: 10.1039/D4NA00652F.
167 L. Zheng, J. Zhang, J. Gao, F. He, S. Yang, H. He, *et al.*, Ratiometric fluorescence sensor based on bimetallic organic frameworks for anthrax biomarker detection, *Biosens. Bioelectron.*, 2025, **278**, 117279.
168 Y. Song, J. Chen, D. Hu, F. Liu, P. Li, H. Li, *et al.*, Ratiometric fluorescent detection of biomakers for biological warfare agents with carbon dots chelated europium-based nanoscale coordination polymers, *Sens. Actuators, B*, 2015, **221**, 586–592.
169 Q. Zhou, Y. Fang, J. Li, D. Hong, P. Zhu, S. Chen, *et al.*, A design strategy of dual-ratiomentric optical probe based on europium-doped carbon dots for colorimetric and fluorescent visual detection of anthrax biomarker, *Talanta*, 2021, **222**, 121548.
170 W. Du, T. Liu, J. Yin, B. Cao, L. Yu, X. Li, *et al.*, Europium-modified carbon dots-based ratiometric fluorescence probe for anthrax biomarker dipicolinic acid detection, *Microchem. J.*, 2025, 114058.
171 M. Rong, X. Deng, S. Chi, L. Huang, Y. Zhou, Y. Shen, *et al.*, Ratiometric fluorometric determination of the anthrax biomarker 2, 6-dipicolinic acid by using europium (III)-doped carbon dots in a test stripe, *Microchim. Acta*, 2018, **185**, 1–10.
172 H. Wu, Q. Wang, L. Zhu, H. Zhang and L. Liu, Regulating the aromatic structure in carbon dots to enhance the internal filter effect for sensitive on-site monitoring of anthrax biomarkers, *Talanta*, 2025, **291**, 127854.
173 H. Chen, Y. Xie, A. M. Kirillov, L. Liu, M. Yu, W. Liu, *et al.*, A ratiometric fluorescent nanoprobe based on terbium functionalized carbon dots for highly sensitive detection of an anthrax biomarker, *Chem. Commun.*, 2015, **51**(24), 5036–5039, DOI: 10.1039/C5CC00757G.
174 M. L. Liu, B. B. Chen, J. H. He, C. M. Li, Y. F. Li and C. Z. Huang, Anthrax biomarker: An ultrasensitive fluorescent ratiometry of dipicolinic acid by using terbium (III)-modified carbon dots, *Talanta*, 2019, **191**, 443–448.
175 Y. Han, H. Wang, Y. Yu, W. Yang, F. Shang and Z. Li, Impact on ratiometric fluorescence of carbon dots hybridizing with lanthanide in determination of residual Carbendazim in food, *Appl. Surf. Sci.*, 2022, **606**, 154700.
176 X. Wang, S. Sun, K. Cheng, T. Lin, H. Wang, H. Sun, *et al.*, Versatile Tb3+–carbon-dot nanoplatform for fluorescence detection and in situ inactivation of bacterial spores, *Sens. Actuators, B*, 2025, **429**, 137296.
177 L. Zhang, Z. Wang, J. Zhang, C. Shi, X. Sun, D. Zhao, *et al.*, Terbium functionalized schizochytrium-derived carbon dots for ratiometric fluorescence determination of the anthrax biomarker, *Nanomaterials*, 2019, **9**(9), 1234.
178 N. Wu, W. Liu, S. Yang, G. Wang, Z. Zhang and S. Guo, Construction of ratio fluorescence sensor based on fluorescence scattering characteristics and its analytical application, *Microchem. J.*, 2025, **213**, 113829.
179 C. Liu, D. Lu, X. You, G. Shi, J. Deng and T. Zhou, Carbon dots sensitized lanthanide infinite coordination polymer nanoparticles: Towards ratiometric fluorescent sensing of cerebrospinal Aβ monomer as a biomarker for Alzheimer's disease, *Anal. Chim. Acta*, 2020, **1105**, 147–154.
180 M. Li, M. Han, X. Song, Y. Chen, Z. Wu, L. Guan, *et al.*, A design strategy of ratiometric optical probe for Fe3+ ions and ascorbic acid detection based on europium-doped carbon dots, *J. Rare Earths*, 2025, DOI: 10.1016/j.jre.2025.10.008.
181 Y. Li, J.-J. Xia, J.-Z. Lu, Z.-L. Wang and M.-T. Wang, Sensitively detection of ascorbic acid in orange samples with ionic liquid functionalized carbon dots and lanthanide complexes, *Dyes Pigm.*, 2024, **227**, 112197.
182 X. Tian and Z. Fan, One-step ratiometric fluorescence sensing of ascorbic acid in food samples by carbon dots-referenced lanthanide probe, *J. Photochem. Photobiol., A*, 2021, **413**, 113261.
183 H. Wang, H. Xing, W. Liu, Y. Hao, L. Zhang, Z. Yang, *et al.*, Gadolinium-doped carbon dots as a ratiometric fluorometry and colorimetry dual-mode nano-sensor based on specific chelation for morin detection, *Sens. Actuators, B*, 2022, **352**, 130991.
184 S. Wei, B. Liu, X. Shi, S. Cui, H. Zhang, P. Lu, *et al.*, Gadolinium (III) doped carbon dots as dual-mode sensor for the recognition of dopamine hydrochloride and glutamate enantiomers with logic gate operation, *Talanta*, 2023, **252**, 123865.
185 J. Duhan and S. Obrai, Lanthanum nitrogen Co-doped carbon quantum dots as optical and smartphone sensors for serotonin detection, *Opt. Mater.*, 2023, **145**, 114466.
186 J. Duhan and S. Obrai, Samarium, nitrogen co-Doped carbon dots for detection of Epinephrine: Theoretical and experimental, *J. Ind. Eng. Chem.*, 2025, **142**, 582–592.
187 Y. Guan, X. Shuai, X. Ruan, Y. Wang and Y. Wei, Both carbon dots precursor and organic bridge ligands for coordination polymers: AMP-based ratiometric fluorescent probes and its application in bovine serum albumin detection, *Int. J. Biol. Macromol.*, 2025, **290**, 139049.
188 F. Algi, M. P. Algi, Ö. Sonkaya and Ş. Ocakçı, Luminescent carbon dots endowed with selective recognition of the carcinoid tumor biomarkers in biological fluids, *Dyes Pigm.*, 2024, **230**, 112333.
189 Z.-H. Chen, X.-Y. Han, L.-X. Deng, Z.-Y. Lin, F.-Y. Mu, S. Zhang, *et al.*, A self-calibrating logic system and oxidase-based biosensor using Tb3+-doped carbon dots/DNA conjugates, *Talanta*, 2019, **191**, 235–240.

190 M. Xu, Z. Gao, Q. Zhou, Y. Lin, M. Lu and D. Tang, Terbium ion-coordinated carbon dots for fluorescent aptasensing of adenosine 5′-triphosphate with unmodified gold nanoparticles, *Biosens. Bioelectron.*, 2016, **86**, 978–984.

191 Y. Guan, Y. Lu and Y. Wei, Fabrication of a ratiometric fluorescent probe based on Tb3+ doped dual-emitting carbon dots for the detection of cytochrome c, *Spectrochim. Acta, Part A*, 2024, **316**, 124310.

192 B. B. Chen, M. L. Liu, L. Zhan, C. M. Li and C. Z. Huang, Terbium (III) modified fluorescent carbon dots for highly selective and sensitive ratiometry of stringent, *Anal. Chem.*, 2018, **90**(6), 4003–4009.

193 L. Liu, C. Zhang, Y. Yu and F. Chen, Determination of DNA based on fluorescence quenching of terbium doped carbon dots, *Microchim. Acta*, 2018, **185**(11), 514.